NASA/CR—1999-209406 ASE 21–10345

Advanced Subsonic Technology (AST) Area of Interest (AOI) 6: Develop and Validate Aeroleastic Codes for Turbomachinery

Kevin D. Gardner, Jong-Shang Liu, Durbha V. Murthy, Marlin J. Kruse, and Darrell James
AlliedSignal Engines, Phoenix, Arizona

Prepared under Contract NAS3–27752

National Aeronautics and
Space Administration

Glenn Research Center

September 1999

Acknowledgments

AlliedSignal Engines would like to thank our Technical Monitor at the NASA-Glenn Research Center (NASA-GRC) Machine Dynamics Branch, Mr. David Janetzke, for his assistance with the programmatic issues in this effort. For the UNSFLO evaluation, we are grateful for the assistance of Dr. Reza Abhari of Ohio State University. In addition, Dr. Dan Hoyniak of Westinghouse provided substantial assistance during our evaluations of the SFLOW code and his advice was greatly appreciated. For the TURBO-AE evaluation, Dr. Milind Bakhle and Dr. Rakesh Srivastava of NASA-GRC provided outstanding support and encouragement which enabled AlliedSignal to successfully complete our evaluation. Finally, we thank Mr. George Stefko of NASA-GRC for his many suggestions, both technical and programmatic, on this effort.

Available from

NASA Center for Aerospace Information
7121 Standard Drive
Hanover, MD 21076
Price Code: A04

National Technical Information Service
5285 Port Royal Road
Springfield, VA 22100
Price Code: A04

TABLE OF CONTENTS

LIST OF FIGURES

LIST OF ACRONYMS AND ABBREVIATIONS

Abbreviation	Definition
AE	AlliedSignal Engines, Phoenix, AZ
AIAA	American Institute of Aeronautics and Astronautics
AL	Alabama
ANSYS®	Finite element analysis code (registered trademark of ANSYS, Inc.)
AOI	Area Of Interest
ASME	American Society of Mechanical Engineers
AST	Advanced Subsonic Technology
AZ	Arizona
CFD	Computational Fluid Dynamics
DAWES	AlliedSignal 3-D Viscous Steady Flow CFD Solver
deg	Degrees
EO	Engine Order
FREPS	NASA-Developed Forced Response Prediction System Aeroelastic Computer Code
GUIde	Government/University/Industry Consortium for Research on Bladed Disks
HP	High Pressure
IBPA	Inter Blade Phase Angle
IR&D	Independent Research and Development
LeRC	NASA Lewis Research Center, Cleveland, OH
MA	Massachusetts
MIT	Massachusetts Institute of Technology, Boston, MA
MSU	Mississippi State University
NASA	National Aeronautics and Space Administration
OH	Ohio
OSU	Ohio State University, Columbus, OH
PA	Pennsylvania
PRDA	Primary Research Development Activity
SET	Small Engine Technology
SFLOW	Steady Flow Solver Computer Program
TFE731	AlliedSignal Engines Turbofan Engine Model
TURBO-AE	NASA/Mississippi State University Developed 3-D Aeroelastic Computer Code
UNSFLO	MIT Developed/AE Modified, Quasi 3-D Aeroelastic Computer Code
U.S.	United States
USAF	United States Air Force
2-D	Two-Dimensional
3-D	Three-Dimensional

ACKNOWLEDGMENTS

AlliedSignal Engines would like to thank our Technical Monitor at the NASA-Lewis Research Center (NASA-LeRC) Machine Dynamics Branch, Mr. David Janetzke, for his assistance with the programmatic issues in this effort. For the UNSFLO evaluation, we are grateful for the assistance of Dr. Reza Abhari of Ohio State University. In addition, Dr. Dan Hoyniak of Westinghouse provided substantial assistance during our evaluations of the SFLOW code and his advice was greatly appreciated. For the TURBO-AE evaluation, Dr. Milind Bakhle and Dr. Rakesh Srivastava of NASA-LeRC provided outstanding support and encouragement which enabled AlliedSignal to successfully complete our evaluation. Finally, we thank Mr. George Stefko of NASA-LeRC for his many suggestions, both technical and programmatic, on this effort.

EXECUTIVE SUMMARY

AlliedSignal Engines (AE), in cooperation with NASA Lewis Research Center (NASA-LeRC), has completed an evaluation of recently-developed aeroelastic computer codes, using two test cases from AE experience: a high-pressure (HP) turbine and a fan integrally-bladed disk ("blisk"). Test data for this task included strain gage, performance, and steady-state pressure information obtained for conditions where synchronous or flutter vibratory conditions were found to occur. The aeroelastic codes evaluated included the quasi three-dimensional (3-D) UNSFLO code, developed at Massachusetts Institute of Technology (MIT) and modified to include blade motion by AlliedSignal; the two-dimensional (2-D) FREPS code, developed by NASA-LeRC and modified by AlliedSignal; and the 3-D TURBO-AE code, under development at NASA-LeRC.

Unsteady pressure predictions from all three aeroelastic codes for the turbine test case were used to evaluate the forced response prediction capability of each code. In addition, one of the fan flutter cases was evaluated using TURBO-AE. The FREPS and viscous UNSFLO predictions showed good agreement with the experimental test data trends, but quantitative improvements are still needed. UNSFLO over-predicted the turbine blade response reductions, while FREPS under-predicted them. Inviscid TURBO-AE turbine analyses predicted no discernible blade response reduction, demonstrating that potential effects are insufficient to capture the dominant physical mechanisms and indicating the necessity of including viscous effects for this test case. Problems encountered in converging the viscous version of TURBO-AE resulted in the decision to model the turbine flow as inviscid.

For the TURBO-AE fan blisk test case, significant effort was expended getting the viscous version of the code to give converged steady flow solutions for the transonic flow conditions in the fan blisk. Once converged, the steady solutions provided an excellent match with test data and the AlliedSignal Engines calibrated DAWES 3-D viscous solver. However, this significant effort focused on a quality steady solution, such that no unsteady results were obtained during the present program. Finally, AlliedSignal recommends that, for both test cases examined, unsteady high-response pressure measurements be made for use in future aeroelastic code validation.

ADVANCED SUBSONIC TECHNOLOGY (AST)
AREA OF INTEREST (AOI) 6:
DEVELOP AND VALIDATE AEROELASTIC CODES FOR TURBOMACHINERY
FINAL REPORT
(CONTRACT NO. NAS3-27752)

1. INTRODUCTION

This Final Report, prepared by AlliedSignal Engines(AE), Phoenix, AZ, and submitted to the National Aeronautics and Space Administration Lewis Research Center (NASA-LeRC), Cleveland OH, summarizes work performed under the NASA Advanced Subsonic Technology (AST) Area Of Interest (AOI) 6: Develop and Validate Aeroelastic Codes for Turbomachinery program. This Final Report covers work accomplished under Contract No. NAS3-27752, during the period November, 1996 through September, 1998. The NASA Technical Program Monitor at NASA-LeRC was Mr. David Janetzke.

The primary objective of the Aeroelastic Codes for Turbomachinery program is to validate Computational Fluid Dynamics (CFD) based aeroelastic analysis tools by comparing simulation results with test data from AlliedSignal Engines turbine engine components. This CFD-based aeroelastic technology will provide critical enhancement to the currently used empirical methods that have been applied successfully at AlliedSignal in the design of numerous gas turbine engines, but have recently been shown to be inadequate for advanced rotor designs such as turbine engine fan bladed disks ("blisks").

Specific CFD-based aeroelastic codes evaluated in this effort included:

- **UNSFLO** (MIT developed, AE modified): a quasi three-dimensional (3-D), viscous unsteady aerodynamic code which allows for blade motion
- **FREPS** (NASA developed): a two-dimensional (2-D) strips, potential steady/unsteady solver, integrated with structural analysis codes
- **TURBO-AE** (NASA development in process): a 3-D viscous solver, integrated with structural analysis codes.

The three codes were evaluated using two test cases based on AlliedSignal designs, as shown in Figure 1. A test case based upon a high-pressure (HP) turbine was used to evaluate the three aeroelastic codes for forced response capability. Additionally, a fan blisk test case was planned to evaluate the flutter prediction capability of the TURBO-AE tool.

Test cases for the code evaluations come from the AlliedSignal Engines fan blisk and HP turbine data bases. Fan flutter was observed during the testing of the selected fan blisk rotor test case, even though empirical correlations had suggested that the design should be "flutter-free". Similarly, synchronous vibrations were observed on the turbine test case, even though the stator-rotor spacing empirical correlations suggested that the design should be acceptable.

These experimental results clearly outline the need for technology improvements in the area of flutter and synchronous response prediction capabilities, and provide strong justification for the continuing leadership provided by NASA in this arena.

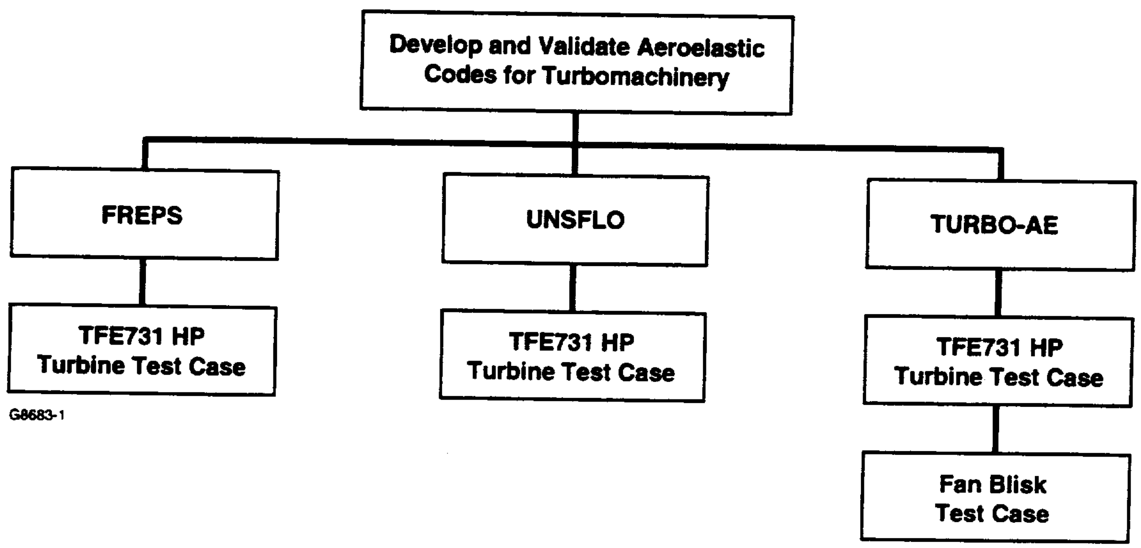

Figure 1. Work Breakdown Structure (WBS) for AOI 6 Aeroelastic Code Validation Effort.

2. BACKGROUND

Since the early 1970s, AlliedSignal Engines has had extensive experience in design, development, and production of turbofan engines for commercial and military applications. The AlliedSignal Engines aeroelastic design approach for these engines has been to apply empirically-based design guidelines to prevent flutter and to minimize synchronous (forced) vibrations. These guidelines have generally proven successful in controlling both flutter and synchronous blade vibrations, thus eliminating the need for more detailed CFD-type analyses.

This continuous focus on designing more efficient and lighter weight turbomachinery has led to the design of damperless, low-aspect-ratio fan blades and turbomachinery blade rows which are squeezed ever closer together to minimize axial length. As a result, testing has shown that the previously-acceptable empirical aeroelastic guidelines do not always provide sufficient margin to prevent flutter or control synchronous vibrations, especially for fans in a blisk configuration having no external damping mechanisms. Under such circumstances, significant engine development program cost and schedule impacts result from the "build and test" iterations required to resolve the aeroelastic issues.

A key technology required to achieve our goal of designing damperless blisk fan rotors and closely-spaced turbomachinery blade rows is the introduction of CFD-type aeroelastic analyses into our design process. AE is working in close coordination with NASA Lewis Research Center to develop this analytical capability. Present aeroelastic prediction methodology at AlliedSignal Engines, described in section 3.0 of this report, was developed under a previous NASA-funded program, Small Engine Technology (SET) Task 8, under Contract No. NAS3-27483.(1)* In addition, AlliedSignal Engines provides internal support through Independent Research and Development (IR&D) and various other engine development programs to enhance aeroelastic prediction capabilities.

* References shown in parentheses ( ) are listed in Section 6.

3. AEROELASTIC METHODOLOGY DEVELOPMENT

As previously mentioned, past aeroelastic analyses by AlliedSignal Engines were based primarily on empirical methods, and CFD-type computations were not completed. This situation is shown in the left side of Figure 2, which outlines the program plan to improve aeroelastic methodology at AlliedSignal Engines. During the 1996-1998 timeframe, AlliedSignal Engines conducted code validation activities under the NASA SET[1] and AST programs. Codes included in this effort include those previously mentioned, plus recently-developed tools from the Government/University/Industry Consortium for Research on Bladed Disks (GUIde).[2] A critical future activity will be to further validate these aeroelastic tools using unsteady pressure measurements from rotors exhibiting flutter and synchronous vibrations. The final goal for all these efforts will be to have a fully-calibrated aeroelastic design system in place for year 2000 engines.

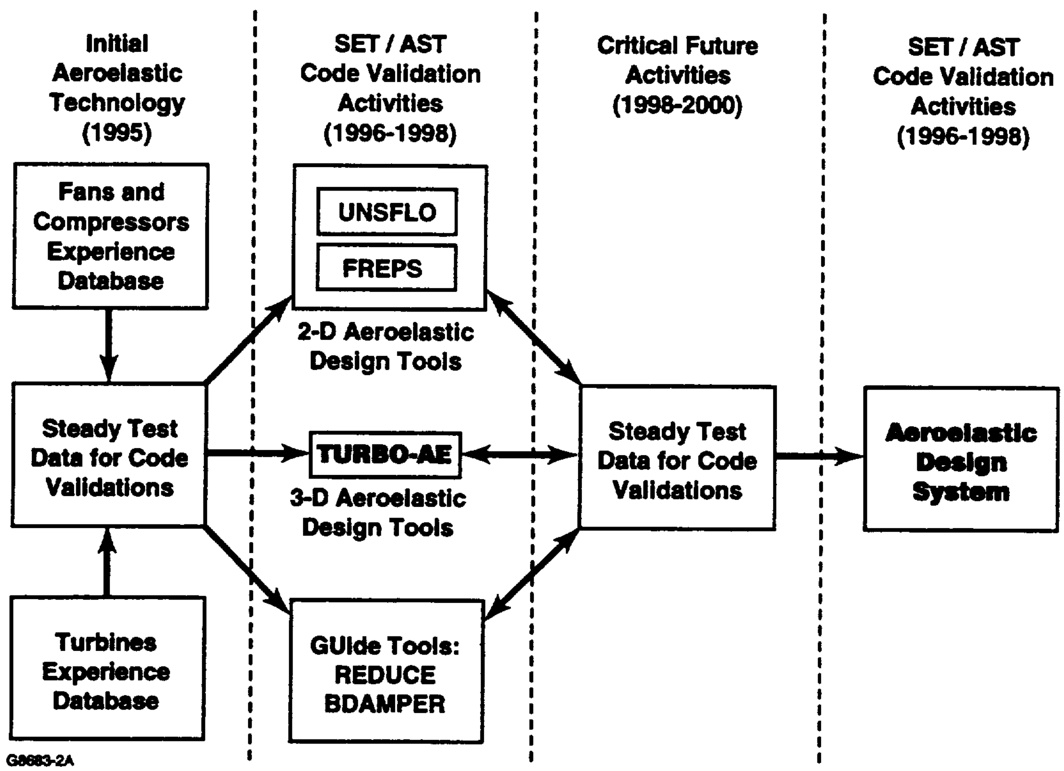

Figure 2. AlliedSignal Engines Aeroelastic Methodology Development Program Plan.

The overall SET and AST aeroelastic methodology development programs are concentrated on both Fan and Turbine code evaluations. This process includes using "steady" test data, which simply consists of operating the codes at conditions (flow, speed, pressure ratio, etc.) where flutter or synchronous vibrations were observed in engine or rig testing. A flowchart of this process is given in Figure 3.

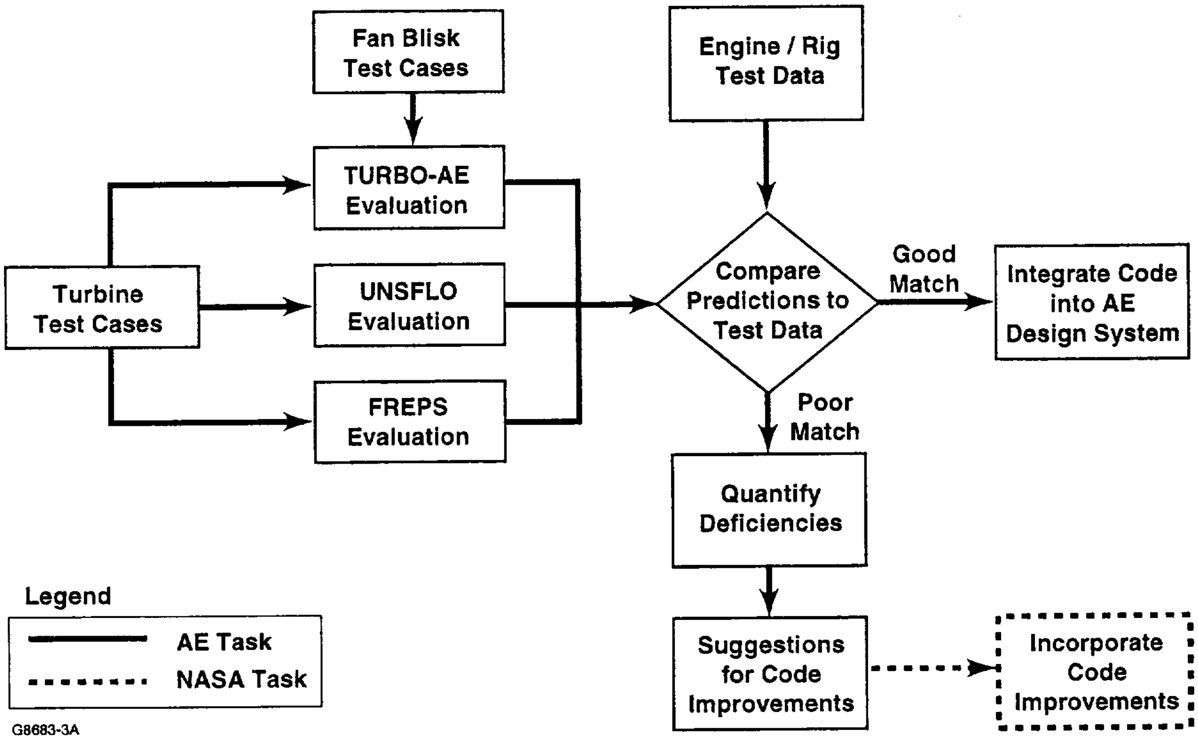

Figure 3. AE SET/AST Code Evaluation Procedure Using "Steady" Test Data.

The basic process is simply to execute the codes and see if the predicted results are consistent with the measured test data from the engine or rig. If the match is good, the code will be directly integrated into the AE design system. When the match is poor, further analysis will be completed to quantify deficiencies and the results will be reported to the code developer for future improvements.

Although validating codes with "steady" test data is the obvious first step, AlliedSignal Engines feels strongly that calibration with "unsteady" data, including blade surface pressures, light probe measurements, and strain gage data, will be required. Two such programs are illustrated in Figures 4 and 5. The GUIde Consortium program at Ohio State University (Figure 4) uses an AlliedSignal Model TFE731-2 HP turbine instrumented with Kulite unsteady pressure transducers and strain gages to obtain unsteady synchronous vibration data. The USAF-sponsored PRDA program (Contract no. F33615-98-C-2922) is an AlliedSignal Engines fan blisk aeroelastic measurement effort, which will provide extensive data in a flutter condition including unsteady pressure measurements on the blade. The test program, to be conducted at the USAF Wright Laboratories Compressor Research Facility, is outlined in Figure 5.

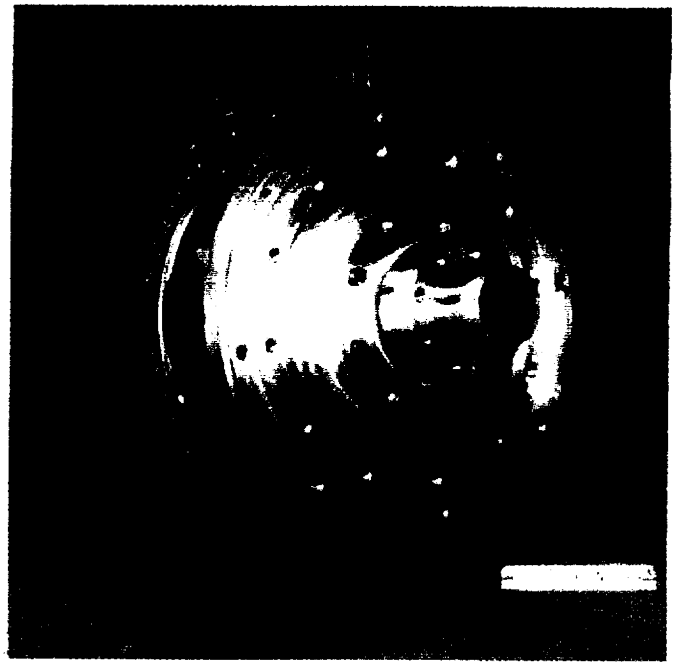

- 41 Upstream Vanes / 78 Rotor Blades
- Subsonic flow conditions
- 4% Field Failure Rate (HCF) prior to redesign
  - Forced Response Vibrations at vane passing frequency
  - 5th Mode (2nd torsion)
  - 19 kHz
- Redesigned rotor eliminated vibration problems

G8683-4

Figure 4. GUIde Consortium Aeroelastic Measurement Program at Ohio State University is Using an AlliedSignal Model TFE731-2 HP Turbine.

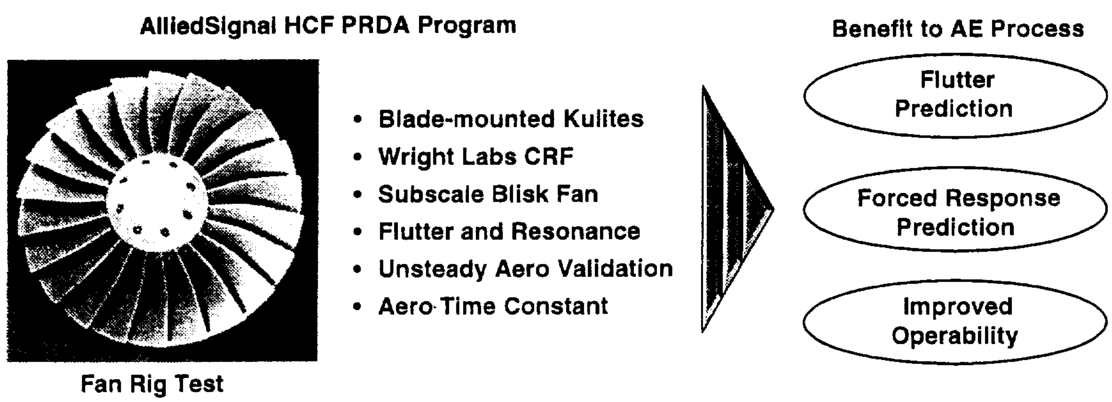

G8683-5

Figure 5. AlliedSignal Engines Fan Blisk Aeroelastic Measurement Program is Being Conducted at USAF Wright Laboratories.

3.1 Development of Execution Procedures for UNSFLO and FREPS

Since AlliedSignal Engines had not completed any CFD-type aeroelastic analyses prior to the NASA-sponsored SET Task 8 program, development of appropriate preprocessors comprised a substantial portion of that program effort.(1) The goal for these preprocessors was to provide a seamless integration with the AE aerodynamic and mechanical design systems. Ease of use is critical in these activities, so the designers who do not regularly perform aeroelastic analyses can easily utilize the tools developed to determine the aeroelastic issues pertinent to the specific rotor configuration.

The process flowchart for integrating aeroelastic analyses with the AlliedSignal Engines aerodynamic design system is shown in Figure 6. Typically, the designer will have either an aero "bankfile" or 3-D steady CFD results from the AE DAWES code available prior to running an aeroelastic analysis. This information will basically consist of the blade and flowpath geometry, along with the flow conditions (pressures, temperatures, velocities, etc.).

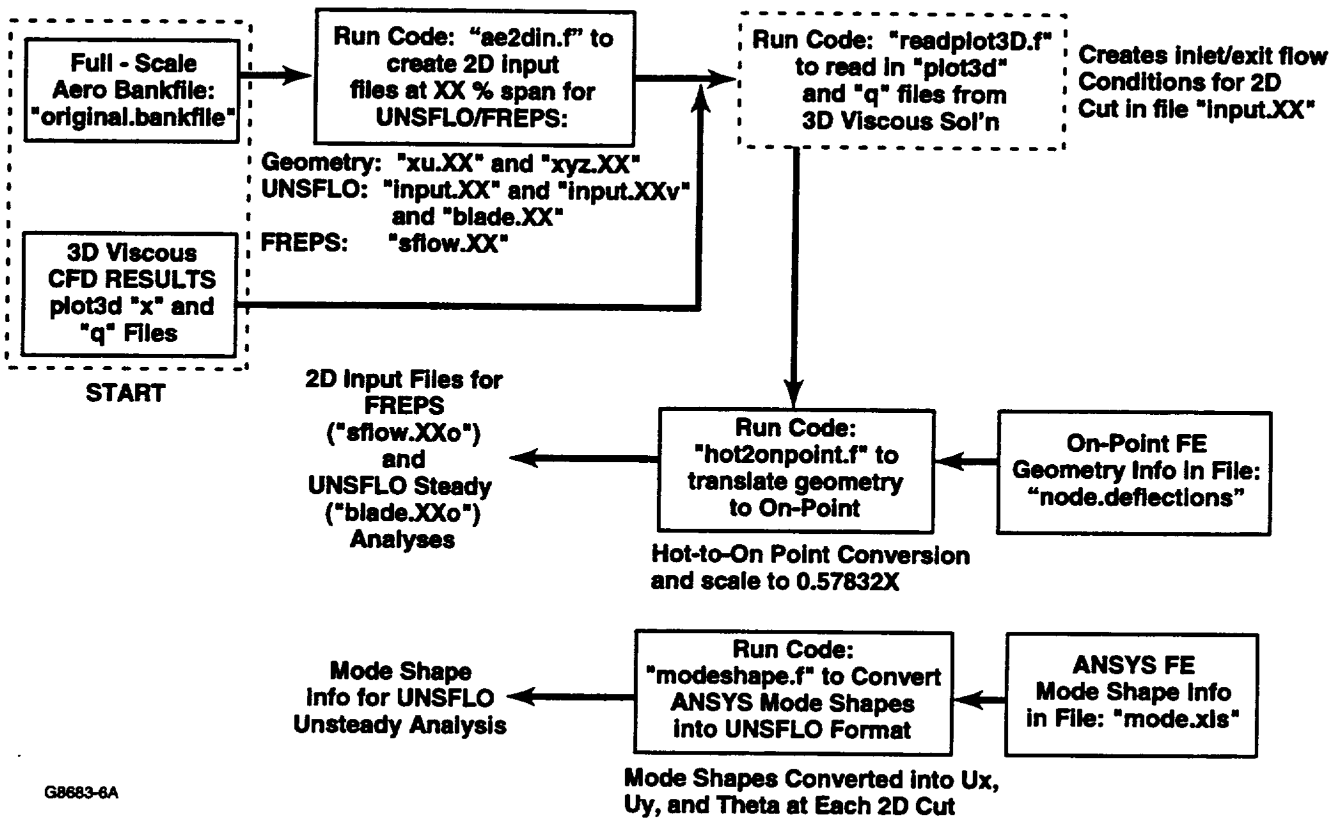

Figure 6. Aeroelastic Analysis Methodology Process (Aerodynamics).

A pre-processor "ae2din" code was developed for UNSFLO and FREPS. This code reads the bankfile and cuts the 3-D geometry into 2-D strips, following either the streamline or the grid line at any user-specified spanwise location. The user has the choice to produce either an UNSFLO or FREPS input file. For an UNSFLO simulation, "ae2din" will create a 2-D geometry file along with the input file which contains the flow information, such as inlet angle, pressure ratio, and Reynolds number. It also creates the stream tube height information based on the 2-D axisymmetric solution in the "bankfile" or the "plot3d" file from any 3-D solutions. For a FREPS simulation, "ae2din" will create one file including the geometry and the flow information.

Following completion of the "ae2din" procedure, the next step in the process is to perform a hot-to-on-point translation which moves the 2-D strip geometry from the "hot" shape used by the aero designers to an "on-point" shape appropriate for aeroelastic analyses at part-speed conditions. The code "hot2onpoint" was created for this process and uses the input file "node.deflections" which is generated from structural finite element analysis. A typical result from this process is illustrated in Figure 7, which shows the difference between the "hot" and "on-point" geometry for a typical test case.

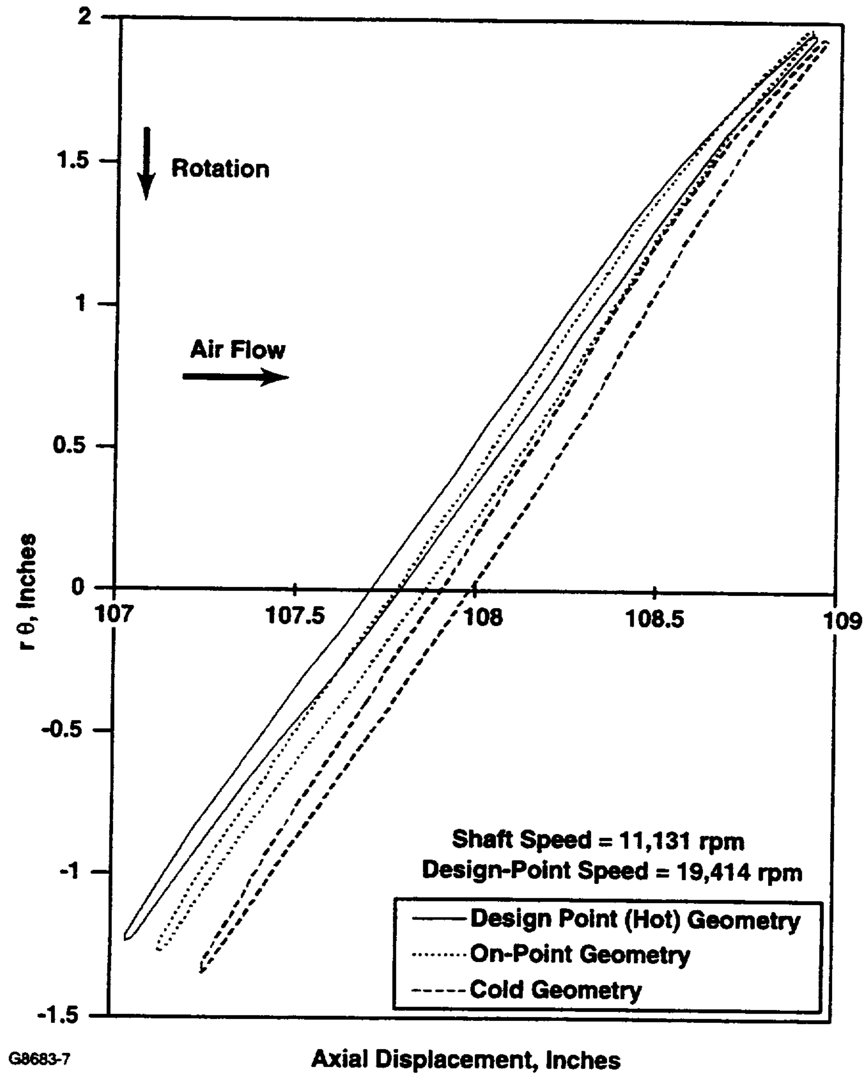

Figure 7. Results From Hot-to-On-Point 2-D Geometry Conversion for Case S1.

The interface of the aeroelastic analyses with the AlliedSignal Engines mechanical design process is outlined in Figure 8. This process again starts with the bankfile and uses the pre-existing code MESHI to generate a structural finite element mesh. The macro "subscale.mac" is then executed to generate a subscale rotor size if required. Next, the user runs pre-existing macros to convert the structural finite element geometry from the "hot" aero shape in the bankfile to "on-point" used in the aeroelastic analyses. The user then runs pre-existing vibratory stress macros to develop the mode shapes for the aeroelastic analyses.

The development of these pre-processors to interface with existing AlliedSignal Engines aerodynamic and mechanical design systems consumed a substantial amount of effort during the prior NASA SET Task 8 program.(1) This effort is expected to pay back several fold, as now the aeroelastic analysis process is reasonably well defined and further improvements will be easy to incorporate.

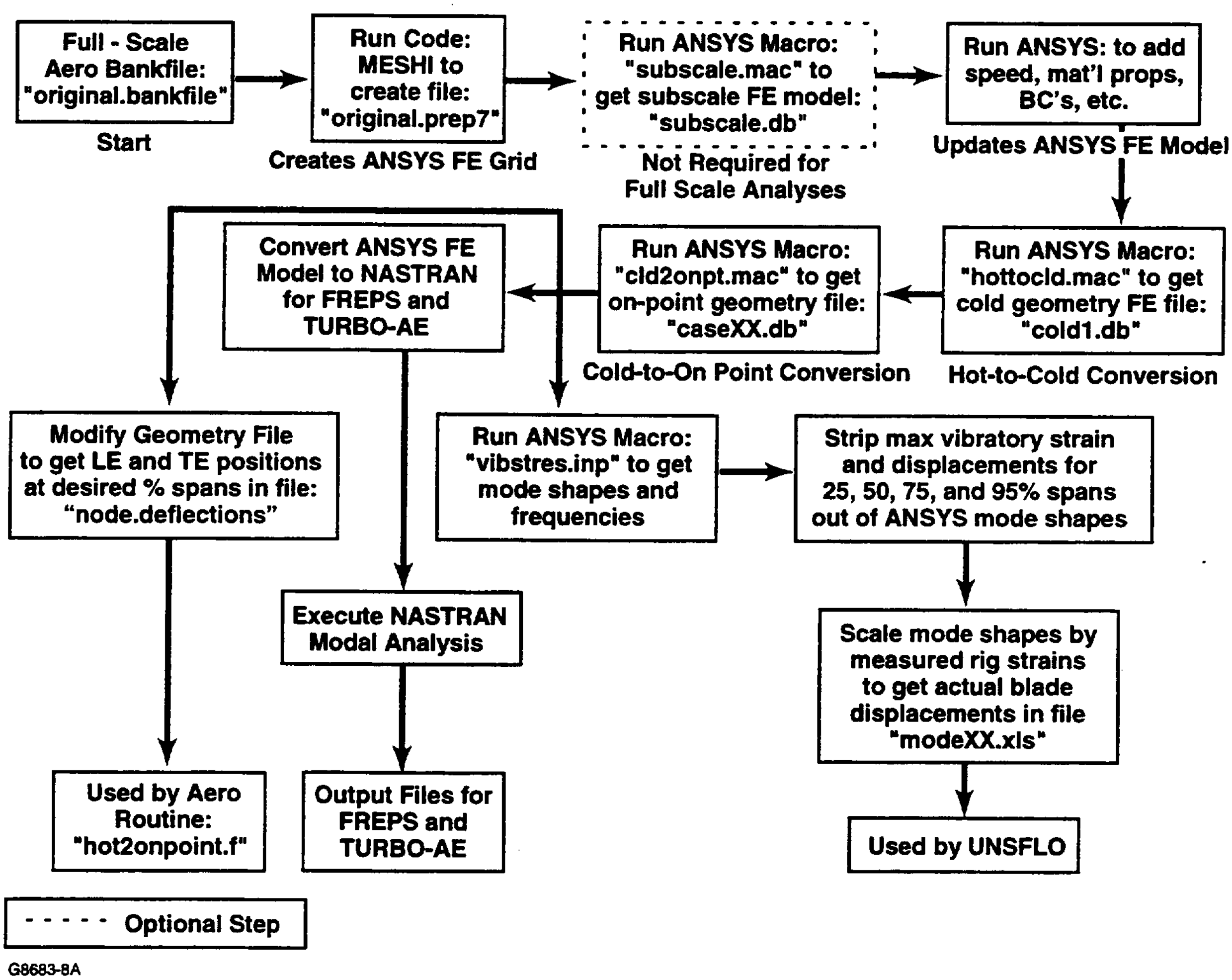

Figure 8. Aeroelastic Methodology Analysis Flowchart (Mechanical).

4. AEROELASTIC CODE EVALUATIONS

During the present NASA AST AOI 6 program, AlliedSignal Engines executed code evaluations for flutter and synchronous vibration cases using the UNSFLO, FREPS and TURBO-AE codes. The test cases used during the evaluation process are described in the following section. Additional sections are included for the UNSFLO, FREPS, and TURBO-AE evaluations.

4.1 Test Case Formulation

Two test cases were used to evaluate the aeroelastic codes. The turbine test case was chosen for its notable synchronous vibratory behavior. The fan blisk test case was chosen for its observed flutter behavior. The test cases are discussed in detail in the following sections.

4.1.1 HP Turbine Test Case

An AlliedSignal high-pressure (HP) turbine rotor which exhibited notable vibration during testing was selected for investigation. The rotor experienced vibrations due to wakes from upstream stator vanes. The rotor consists of 78 uncooled blades inserted into a disk through a firtree attachment, as shown previously in Figure 4. The upstream stator consists of 41 vanes that generate wakes, causing the downstream turbine blades to vibrate. A 3-D solid model of the stator-rotor configuration is shown in Figure 9.

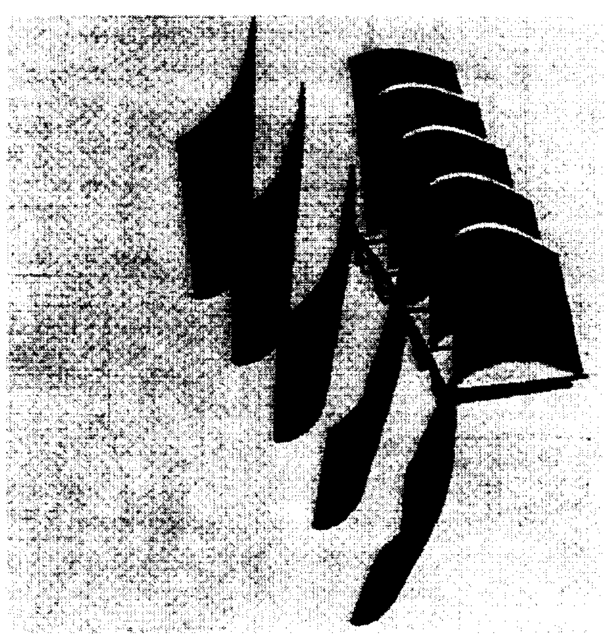

G8683-9

Figure 9. 3-D Solid Model of the Stator-Rotor Configuration for the HP Turbine Rotor Test Case.

A Campbell diagram for the HP turbine test case indicates the participation of the first bending and second torsional modes in the vibratory response, as shown in Figure 10. The response, however, is dominated by the second torsional mode, as indicated in Figure 11. The second torsion mode crosses the 41st engine order (EO) at approximately 93 percent of full speed.

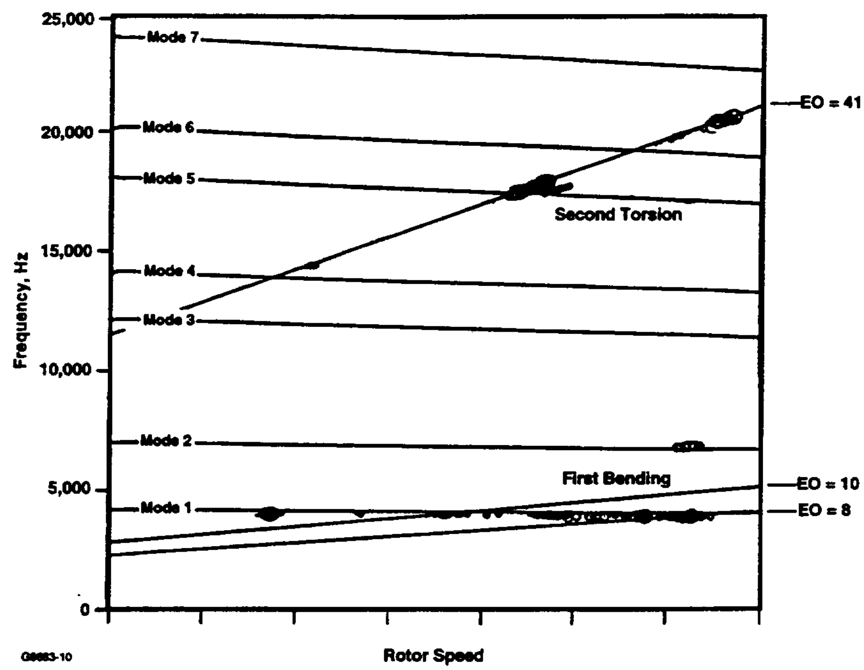

Figure 10. Campbell Diagram For The HP Turbine Blade.

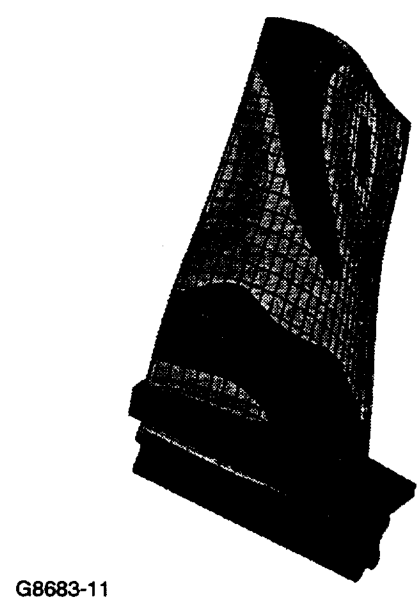

Figure 11. Second Torsional Mode Shape.

Two different stator-rotor spacings were evaluated during the testing. The baseline, closely-spaced configuration exhibited significant vibrations during engine testing. The distance separating the trailing and leading edges in the baseline configuration is approximately 50 percent of the rotor tip chord. Measured test data shows vibratory strain levels decreased 45 to 72 percent when the axial spacing was increased to 70 percent of the rotor tip chord.

4.1.2 Fan Blisk Test Case

An AlliedSignal Engines advanced technology integrally-bladed fan rotor disk ("blisk"), which exhibited flutter during rig testing, was selected for investigation. The fan blisk, shown in Figure 12, is a 22-bladed damperless rotor with an advanced, swept airfoil designed for optimum performance and minimum weight.

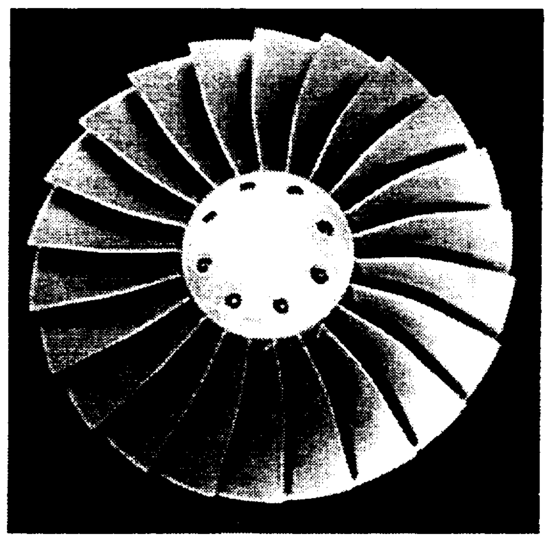

G8683-12

Figure 12. AlliedSignal Integrally-Bladed Fan Rotor Blisk Was Evaluated.

The fan performance map, Figure 13, shows six test conditions, labeled F1 through F6, where flutter was observed. The flutter cases all occurred with clean inlet operating conditions on the test rig; i.e., no distortion screens were required to initiate or sustain the flutter. Two additional test cases, labeled NF1 and NF2, were developed to test the codes at conditions where flutter was not observed during testing. These cases correspond to the design point for the fan rotor. The flutter cases, F1 through F6, are divided into two zones: low speed (F2, F4, F5, and F6) and high speed (F1 and F3).

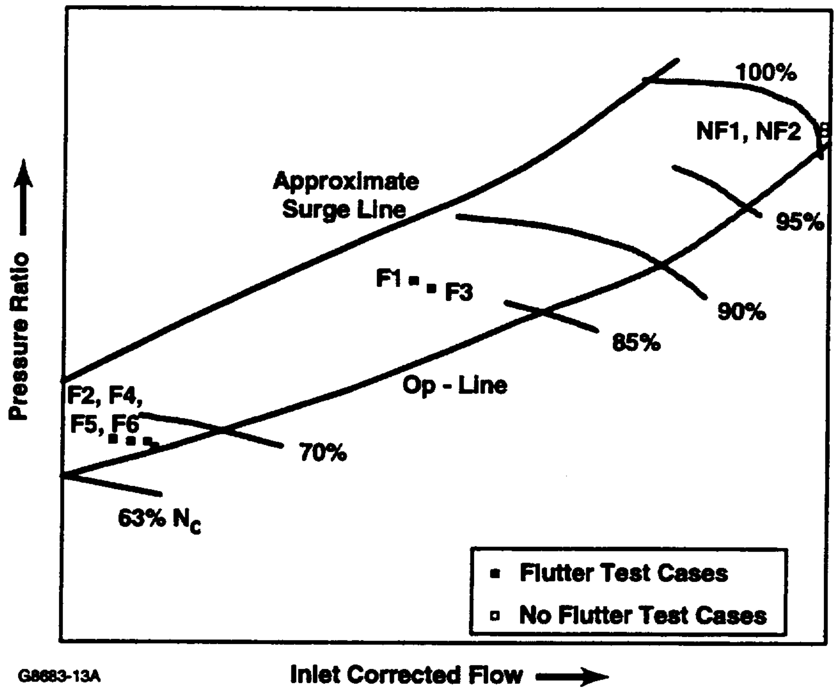

Figure 13. Fan Blisk Performance Map.

Spectrum analysis of the strain gage signals indicated that the flutter vibration frequency corresponds to the first flexural mode of the airfoil for all the test cases F1 through F6. Detailed structural finite element analyses using the ANSYS® code[3] revealed that the airfoil leading edge displacement is approximately twice that observed at the trailing edge, indicating that the first flexural mode has a significant torsional component. This situation can be seen from Figure 14, which shows the vibrational mode shape for test case F2 computed for a fixed-root airfoil. It should be noted that the mode shape displacements shown in Figure 14 represent the vector sum of the three (x, y, z) displacement components.

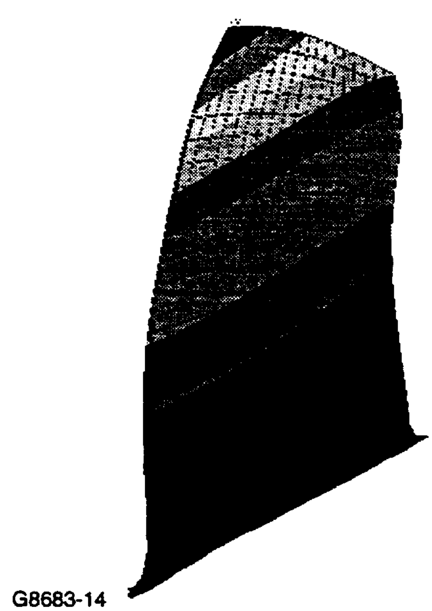

Figure 14. Normalized Vibrational Mode Shape for Case F2.

4.2 UNSFLO Code Evaluation

4.2.1 General

To evaluate the UNSFLO code, AlliedSignal Engines compared experimental observations from a pair of high-pressure turbine tests against forced-response predictions from UNSFLO and ANSYS®. UNSFLO was used to characterize the unsteady flow fields, and ANSYS® was used to predict the turbine blade structural response to the unsteady flow field. The HP turbine under investigation (see Section 4.1.1) exhibited significant blade vibratory response, due to pressure waves and wakes from upstream stator vanes. Experimental data was collected on two stator-rotor configurations. The first configuration, built with a close axial spacing, was found to have high levels of vibration during testing. The distance separating the trailing and leading edges was approximately 50 percent of the rotor axial tip chord. Vibratory strain levels dropped substantially for the second configuration, in which the spacing was increased to 70 percent of the rotor axial tip chord. The objective of this analysis was to determine if the UNSFLO/ANSYS® combination could match the experimental observations.

4.2.2 UNSFLO Code Description

UNSFLO is a quasi 3-D, Reynolds-averaged, unsteady multi-blade row Navier-Stokes solver developed by Giles.(4) Specific details on the theory and formulation of the UNSFLO code can be obtained from the references, so only an overview will be presented here.(4, 5, 6)

UNSFLO couples an inviscid solution of the Euler equations in the outer region to a Navier-Stokes solution in the shear layer near the airfoil. Quasi 3-D effects are included through the addition of streamtube height in the third dimension. The inviscid grid used in these analyses is a structured H-type mesh, while the viscous computations use an O-grid wrapped around the airfoil. A Baldwin-Lomax algebraic turbulence model is used in the viscous part of the solution.

To simulate rotor-stator interaction, UNSFLO uses a unique "time-tilting" technique to accommodate uneven blade counts for the stator and rotor. If the pitch ratio between two stator-rotor blade rows is too large (i.e., greater than 1.5), the time-tilting technique breaks down and two or more passages are needed to obtain a smaller pitch ratio. For the current stator-rotor analysis, the computational domain contains one stator passage and two rotor passages. The pitch ratio between the stator and rotor is 39/41 (= 0.95).

4.2.3 Analysis Methodology

A flowchart of the UNSFLO/ANSYS® analysis is shown in Figure 15. After formulating the test case objectives, the first step in the analysis is to determine separate steady flow solutions for both the stator and rotor blades. The steady solution sets are then used as starting solutions for the combined stator-rotor analysis. Once complete, postprocessing of the unsteady solution yields the pressures acting on the vane and blade surfaces at equally spaced time intervals in a single vane passing period. UNSFLO analyses were completed at four radial spans (25, 50, 75, and 85 percent span).

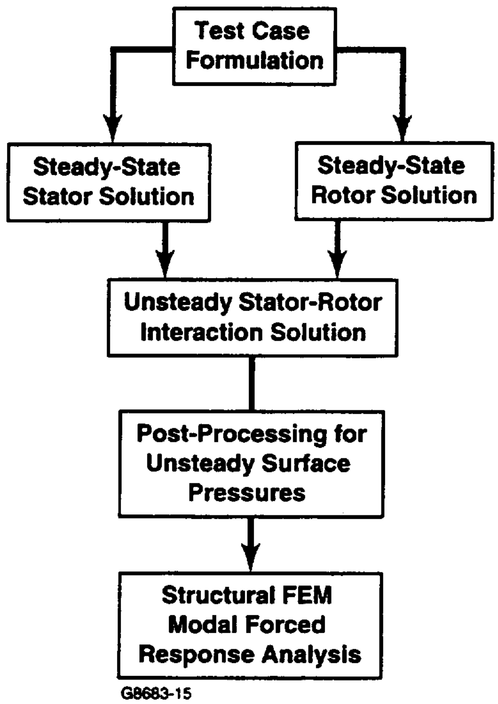

Figure 15. UNSFLO Analysis Flowchart.

The unsteady blade surface pressures are then mapped onto a structural finite-element model. Pressures are linearly interpolated between known CFD solution spans, with linear extrapolation occurring for structural elements outside the CFD solution region. Forced-response modal calculations are then performed in ANSYS® to obtain the vibratory strain amplitudes. Damping estimates were obtained from the Forced Response Prediction System (FREPS),[7, 8] which is a coupled structural dynamics and aerodynamics code. Modal damping equivalent to 2.0 percent critical damping is assumed for all forced-response calculations.

Note that the UNSFLO analyses do not include blade vibration. Only motion due to rotation (stator-rotor interaction) is included. The impact of this simplification on the unsteady flow solution of the blade motion is not known at the present time.

Computation times for the UNSFLO unsteady flow analysis are approximately four hours per radial span. This fast turnaround allows a forced response analysis to be completed in an overnight fashion, simply by running each span on a different workstation.

4.2.4 UNSFLO Results

4.2.4.1 Computational Grid

The computational grid used in the UNSFLO analyses includes both the vanes and the rotor, as shown in Figure 16. In the outer region, away from the airfoils, the grid is an H-type and the Euler equations are solved. Near the airfoil surfaces, the mesh is an O-type and the Navier-Stokes equations are solved.

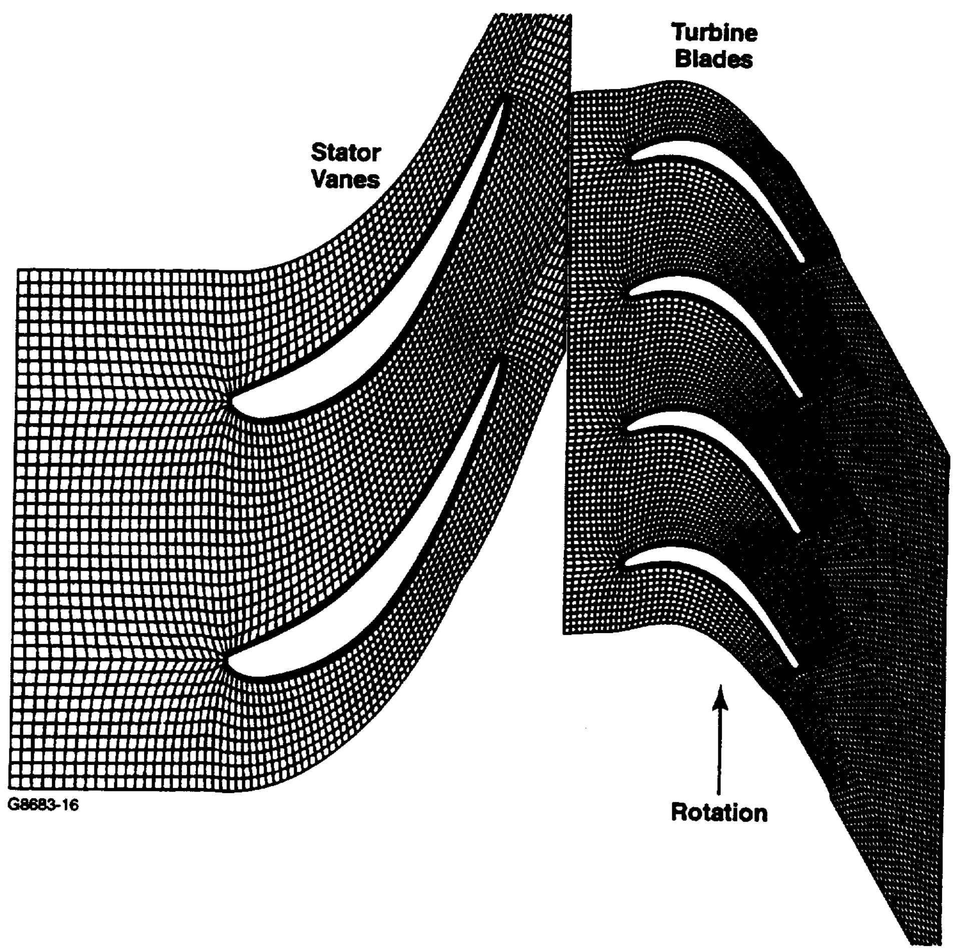

Figure 16. UNSFLO Computational Grid at 85 Percent Span.

4.2.4.2 Unsteady Flow Comparisons

The unsteady flow solution is obtained by running UNSFLO in the stator-rotor configuration for 6,000 iterations until the code converges, as shown in Figure 17.

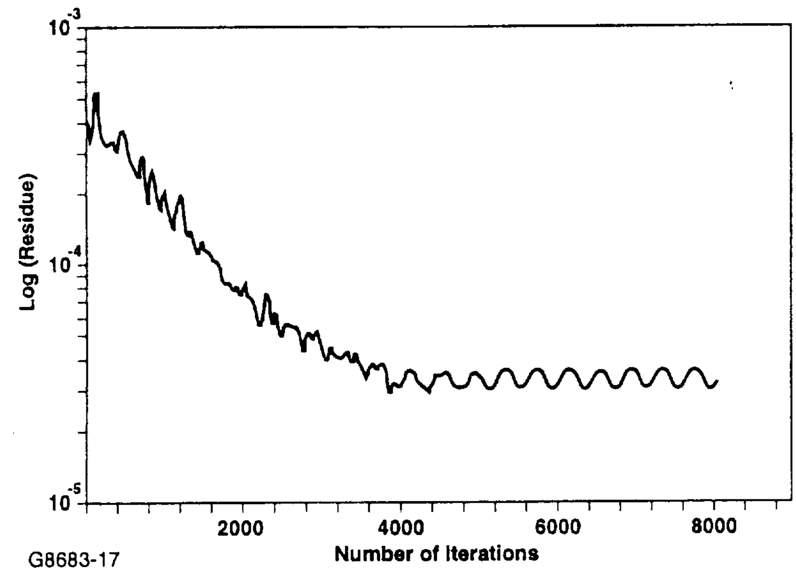

Figure 17. Typical UNSFLO Residual Convergence.

Mach number contours for the two stator-rotor spacings are shown in Figure 18 at one-quarter excitation period intervals. The contours on the left side of the figure correspond to the close stator-rotor spacing case, while the contours on the right side correspond to the enlarged stator-rotor spacing case. As shown in Figure 18, the stator pressure wake impinges directly on the rotor blade leading edge for the close spacing case. When the stator-rotor gap is increased, the stator pressure wake is more diffuse, thereby decreasing blade excitation.

Unsteady pressure envelope predictions from UNSFLO for both small and large stator-rotor axial spacings are shown in Figures 19(a) and (b), respectively. Large peak-to-peak amplitude variations dominate the small stator-rotor spacing design. The pressure variations lead to principal strain levels that are 90 percent lower than the small spacing design. Experimental measurements, in comparison, indicate a 45 to 72 percent decrease in strain amplitude with the enlarged stator-rotor spacing design.

(A) Time = 0.000

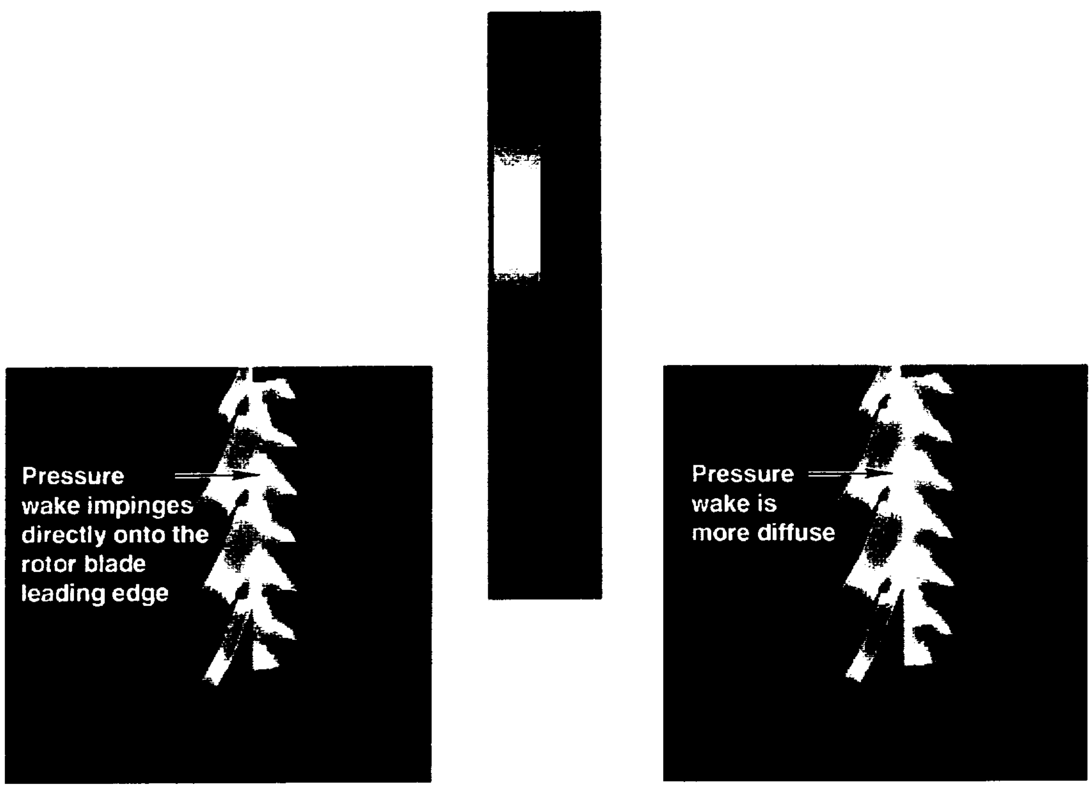

G8683-18-1

(B) Time = 0.250

Figure 18. Mach Number Contours Illustrate the Location of Pressure Wakes for Small (Left) and Large (Right) Stator-Rotor Axial Spacing Configurations.

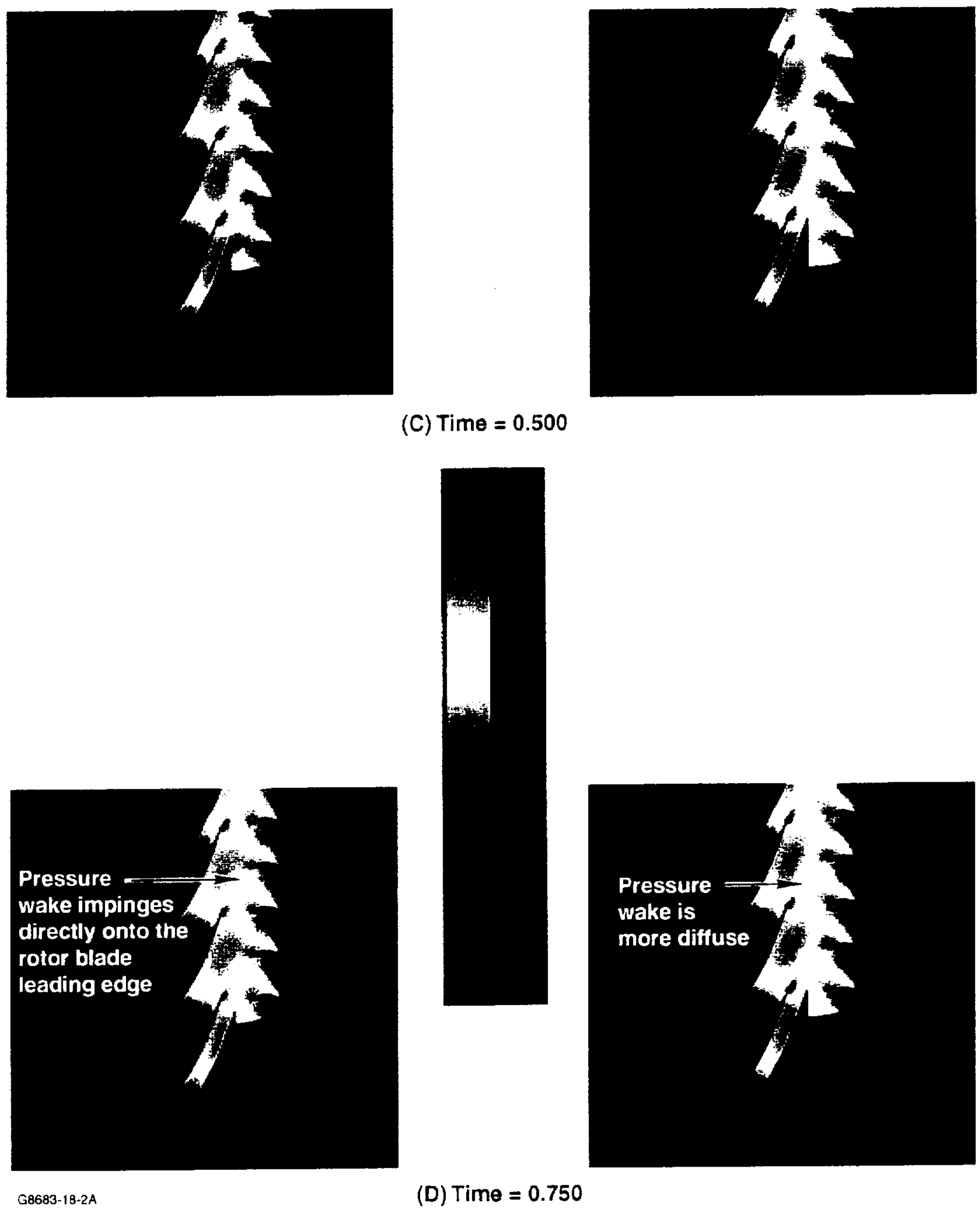

Figure 18. Mach Number Contours Illustrate the Location of Pressure Wakes for Small (Left) and Large (Right) Stator-Rotor Axial Spacing Configurations (Contd).

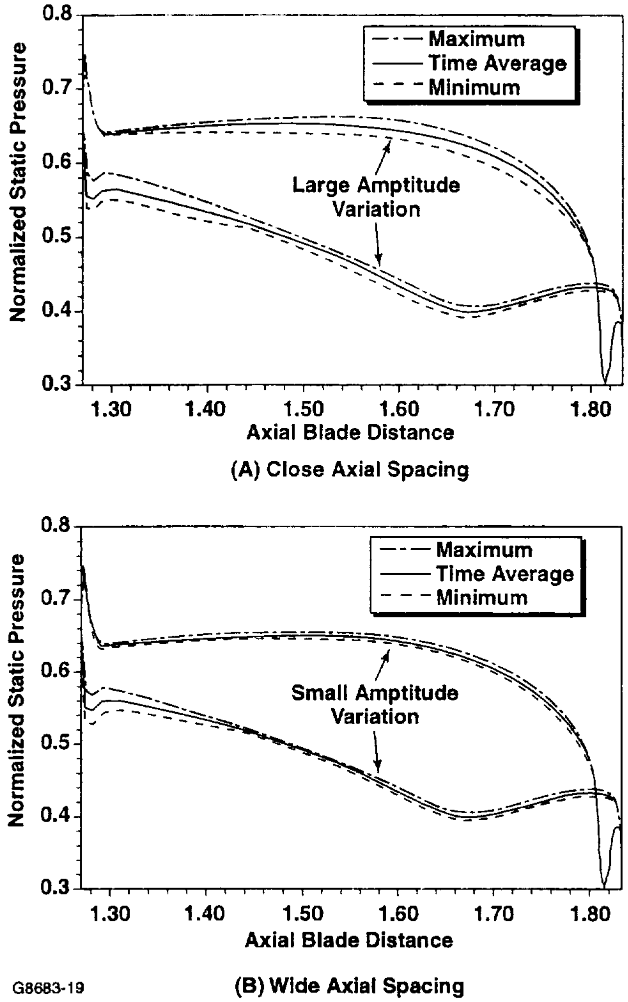

Figure 19. UNSFLO Pressure Distribution Plots.

4.2.5 Conclusions – UNSFLO Evaluation

This work demonstrates the successful integration of UNSFLO with the structural dynamics code ANSYS® for the HP turbine test case. Coupling of the codes is accomplished by mapping unsteady pressures at discrete radial spans onto a structural finite element model. Pressures are linearly interpolated between known CFD solution spans, with linear extrapolation occurring for structural elements outside the CFD solution region. Computer simulations of two axial stator-rotor spacing configurations indicate a 90 percent reduction in vibratory strain. The software predictions agree favorably with experimental observations of a 45 to 72 percent reduction in vibratory strain. It should be noted that experimental testing revealed no significant change in overall engine performance with the spacing change. This work demonstrates that current CFD codes, such as UNSFLO, can predict the aeroelastic implications of various design changes and that integration of two previously autonomous fields, computational fluid dynamics and structural dynamics, will aid future turbomachinery designs.

4.2.6 Recommendations for Further Development of the UNSFLO Code

During the course of the present effort, AlliedSignal Engines obtained substantial experience operating the UNSFLO code. Several areas for improvement and further study have been suggested and are summarized as follows:

- Develop improved inlet distortion and wake modeling capabilities for synchronous vibrations.
- Add a feature to incorporate blade motion into unsteady analyses for multi-blade row cases.
- Experience obtained applying UNSFLO for flutter analysis outside the scope of this AST program reveals that, while unsteady analyses are the critical element to flutter analyses, steady analyses are the current barrier to using UNSFLO. AE suggests developing a more robust steady state solver to replace the current steady analysis in UNSFLO.

These recommended changes will greatly improve the capabilities of the UNSFLO computational tool.

4.3 FREPS Code Evaluation

4.3.1 General

In the FREPS code evaluation element of the AOI 6 program, AlliedSignal Engines implemented a version of FREPS that is compatible with ANSYS® and the latest versions of the steady aerodynamic code SFLOW and the unsteady aerodynamic code LINFLO. AE also validated the FREPS system comparing the predicted forced response on the turbine rotor with test data. AE's efforts in this task have enhanced the FREPS program substantially. A process was also developed to compute the harmonic gust excitation from the UNSFLO rotor-stator analysis.

4.3.2 FREPS Code Description

The FREPS system integrates a structural dynamics analysis with steady and unsteady aerodynamic analyses to perform an aeroelastic analysis. Each analysis (structural, steady, and unsteady aerodynamic) is completed separately and input into the FREPS integration package. The different analysis modules communicate with one another through binary database files. The structure of these database files is quite complex, and this is a major factor in the time it takes to implement new versions of steady and/or unsteady aerodynamic modules.

The execution of FREPS requires running ANSYS® to get blade frequencies and mode shapes, SFLOW to establish a steady aerodynamic solution, running LINFLO to build a grid for unsteady analysis, and finally, running FREPS to perform aeroelastic analysis. FREPS calls LINFLO several times to perform unsteady aerodynamic analysis. The procedure is illustrated in Figure 20.

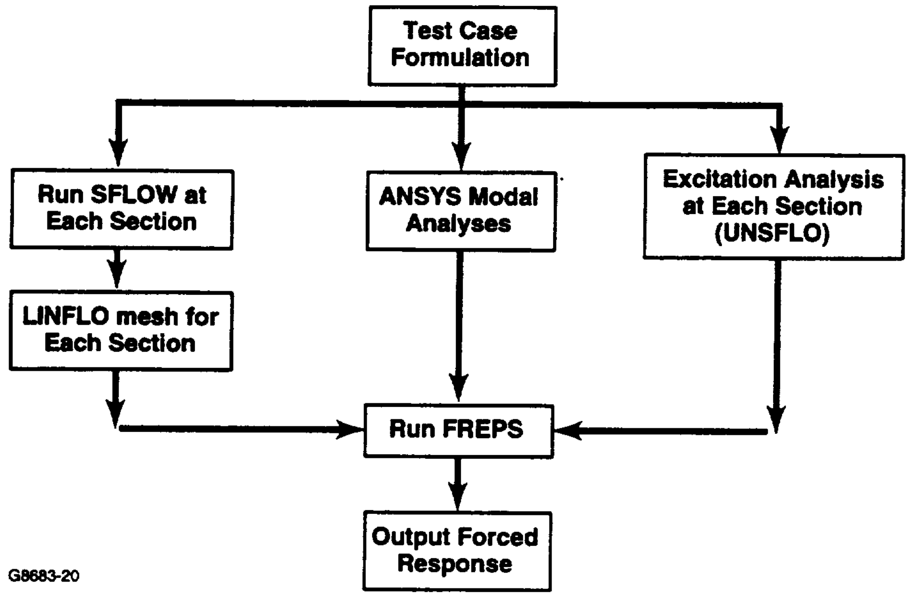

Figure 20. The FREPS System Process.

4.3.3 FREPS Code Revisions by AlliedSignal Engines

Several changes were implemented by AlliedSignal Engines to the FREPS aeroelastic analysis computer program. As suggested by the NASA Contract Monitor on the AST program, this revised version of FREPS is designated as Version 2.0. Nearly all the changes were introduced to make the FREPS program compatible with the following programs:

- Finite element analysis program, ANSYS® ,Version 5.4
- Steady flow analysis program SFLOW, Version 1.7
- Unsteady flow analysis program LINFLO, Version 1.5.

The following is a summary of the changes to FREPS implemented by AlliedSignal Engines:

1. An interface with ANSYS® structural dynamic analysis has been implemented.
2. The FREPS system has been modularized to better separate unsteady aerodynamic and aeroelastic calculations. The aeroelastic module of the FREPS system has been stripped of all routines common to the unsteady aerodynamic modules. This makes the process of replacing the current version of LINFLO in the FREPS program with newer versions easier and more reliable. However, the modularization is not sufficient to easily replace LINFLO with an unsteady aerodynamic code of a very different structure. These comments also apply to the steady aerodynamic code, though to a lesser extent. The aeroelastic module reads the steady flow only for documentation purposes.

3. Include files have been made compatible among SFLOW Vers. 1.7 and LINFLO Vers. 1.5.
4. The definitions of leading and trailing edges and upper and lower surfaces have been streamlined throughout the code.

4.3.4 FREPS to ANSYS® Interface

The original FREPS Version 1.2 code had an interface with MSC/NASTRAN(9) for reading blade 3-D geometry, structural dynamic model, and results. A similar interface with ANSYS® has been developed in (the AlliedSignal revised) FREPS Version 2.0. The specification of the FERESULT record is now changed. The revised specification is given below (in Figure 21) which can be used to substitute for (the original) page 2.2-15 of the FREPS User's Manual (NASA CR-194465).(7)

4.3.5 Additional FREPS Changes by AlliedSignal Engines

Additional FREPS changes made by AlliedSignal Engines are summarized as follows:

1. The FREPS code has been repackaged to include SFLOW and LINFLO within one tar file and the makefile contained therein. The whole package can now be treated as one single program for the purposes of acquisition and compilation. However, the execution of SFLOW and FREPS is still independently controlled by separate executables.
2. The following include files have been modified for compatibility with the database definition in the new versions of SFLOW and LINFLO:

   gastrm

   gausdt

   pmprmb

   raqira

   rmprmc

   ucprmu
3. Problems dealing with scratch files have been fixed in subroutines READFE and STDFLO.
4. The subroutine GENEXC, which processes the blade motion obtained from the mode shape, has been extensively modified to be compatible with the new versions of SFLOW and LINFLO.
5. FREPS Version 1.2 will stop execution if the x-coordinate of the trailing edge is less than that of the leading edge. In the revised FREPS Version 2.0, execution proceeds, with a warning issued in the printout.

FERESULT **Finite Element Database File**

Description:

The FERESULT record defines the type of finite element output and the file name of the output results.

Format and Example:

FERESULT Fetype filename

FERESULTS NASTRAN mscnast.out

Field Description:

Field	Name	Type	Description
1	FERESULT	Character	Mnemonic name
2	Fetype	Character*20	Finite element output type: NASTRAN = MSC/NASTRAN ANSYS = ANSYS
3	FILENAME	Character*20	Unix file name of the output

Notes:

1. Currently, NSC/NASTRAN and ANSYS are the only FE solvers supported in Version 2.0 of FREPS.

Figure 21. Revised FERESULT Procedure. (Ref: Page 2.2-15 of FREPS Users' Manual.)

6. Due to the extensive incompatibilities, sound pressure calculations in subroutine **ntrprt** have been commented out, as it was felt that they are of no interest to aeroelasticians. The program prints out the following message:

   All sound pressure level calculations skipped!

7. The subroutine READLN, which reads the input files, has been modified to accept tab characters as field delimiters, in addition to spaces and commas.
8. The subroutine MASSAGE has been changed to MASSAGENEXC.
9. The include statement syntax has been changed to the following syntax:

   include 'xxxxxx'

   Instead of:

   #include "xxxxxx".

   The above format is compatible with the f77 compiler on HP-UX. A Unix script has been developed to easily switch between the two include statement formats.
10. Common block references throughout the code have been streamlined, so that all common blocks with the same name contain the same variables in the same order.
11. The output from the FREPS code has been substantially improved in readability by adding additional information and removing debugging–type write statements.
12. The description of the format of the finite element output has been improved by adding comments to the subroutine READFE that describe the format in detail.
13. MSAVE and MPRINT settings have been changed in subroutine LINFLO.
14. Minor "bugs" have been fixed in subroutines **cdp_bbn**, **linflo**, **pres** in LINFLO.
15. All **lapack** routines have been separated into the directory **lapack** and compiled into the library **lapack.a**.
16. All acoustic calculations have been disabled, because the compatibility of these calculations with the new versions of SFLOW and LINFLO has not been checked.

4.3.6 Validation Results

For the two-dimensional aerodynamic analysis, the blade was divided into four strips centered at approximately 25, 50, 75, and 85 percent span locations. A sharp trailing edge was used in the aerodynamic meshes to properly enforce the Kutta condition. The same steady-flow solution was used for both baseline and enlarged rotor-stator spacing conditions.

4.3.6.1 Aerodynamic Computations

The steady aerodynamic analysis is performed using the steady, full potential flow solver SFLOW, Version 1.7. This solver uses the non-conservative form of the nonlinear potential flow equations, together with an implicit, least-squares, finite-difference approximation to solve for the steady-flow field around a given isolated, infinite cascade of identical airfoils. A composite mesh, consisting of a global H-mesh (92 x 31) and a local C-mesh (89 x 11) as shown in Figure 22 is used. The global mesh is intended to capture blade-to-blade aerodynamic phenomena, and the local mesh, to resolve high-gradient phenomena in the region of blunt leading edges.

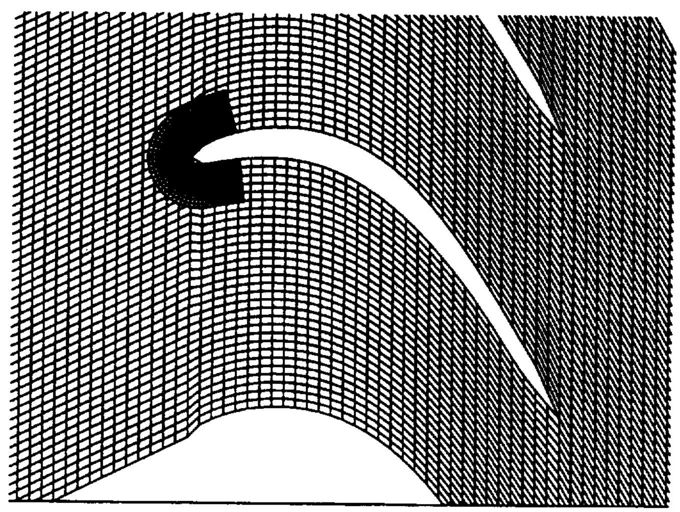

G8683-22

Figure 22. Composite Mesh For Steady Flow Solution.

The steady aerodynamic calculations were performed using the inlet flow angles and Mach numbers predicted by UNSFLO rotor-stator analysis as boundary conditions. Figure 23 shows the typical distribution of the mass flow in the axial direction. It shows that the conservation of mass has been satisfied very well, in contrast to the deviations seen in earlier calculations.

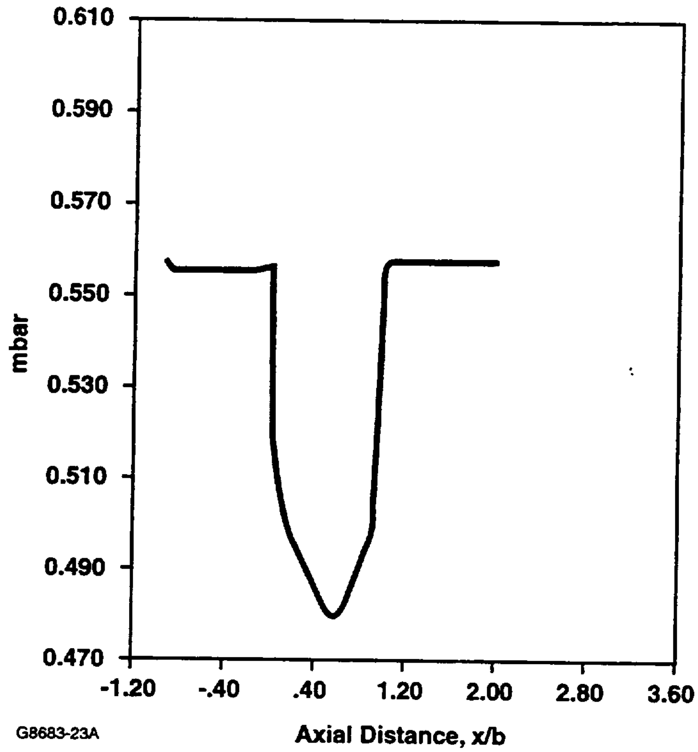

Figure 23. Typical Distribution Of Mass Flow In Axial Direction.

The steady Mach number distribution calculated is shown in Figure 24. This figure is typical of the results for all the sections. The Mach number contours appear to be quite smooth and the solution is well converged. The unsteady aerodynamic flow was computed using LINFLO and the 150 x 40 streamline mesh depicted in Figure 25.

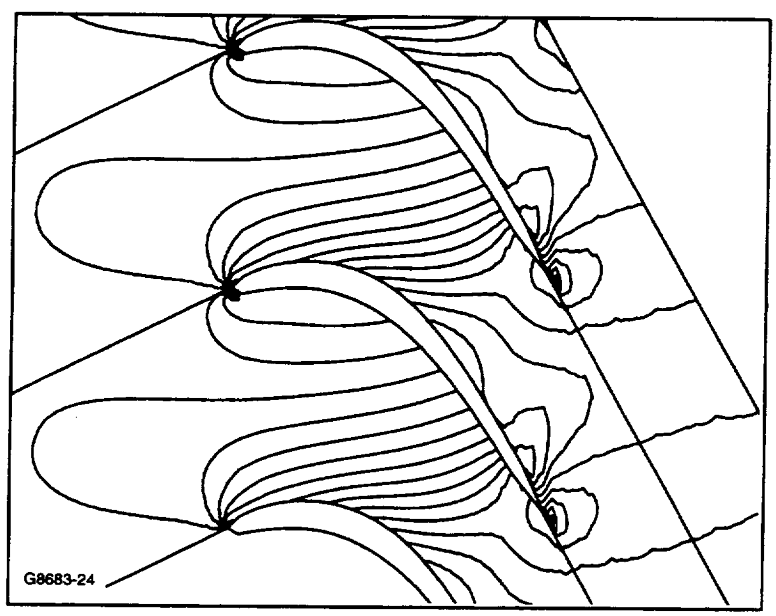

Figure 24. Typical Mach Number Contours.

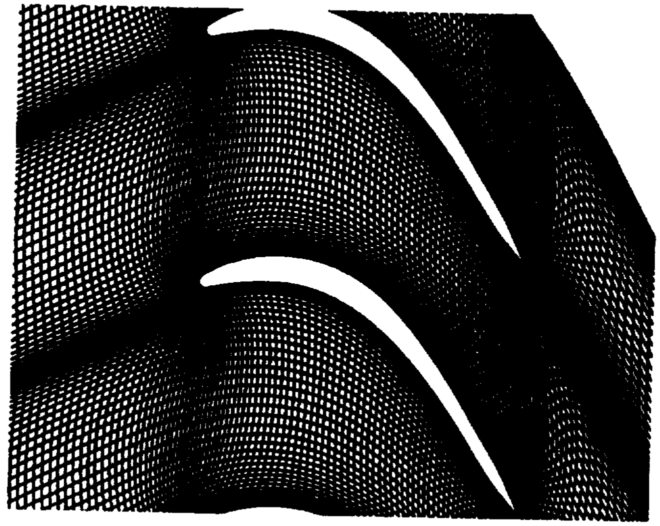

Figure 25. LINFLO Grid For Unsteady Solution.

4.3.6.2 Aeroelastic Computations

The aeroelastic calculations were performed for baseline and enlarged rotor-stator spacings, assuming single-mode excitation and response and a modal damping ratio of 0.2 percent. The excitation was obtained from UNSFLO rotor-stator analysis detailed in section 4.2 of this report. Only the fundamental harmonic of the excitation, which causes resonance in the fifth mode (18,752 Hz) of the turbine blade was used, because the modal density was low at this speed.

The mode shape corresponding to this mode was calculated with ANSYS® and imported into FREPS using the new FREPS-ANSYS® interface. The mode shape contours are shown in Figure 26.

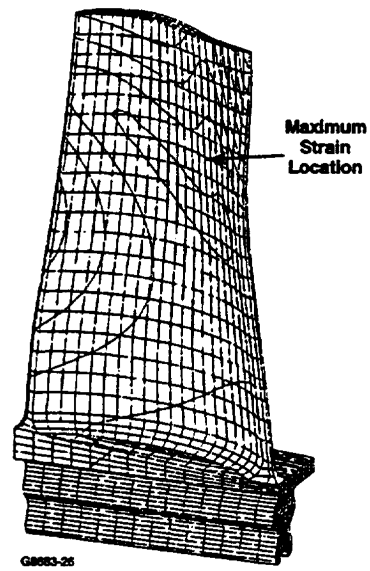

Figure 26. Fifth Vibrational Mode Shape.

For these cantilevered blades, the loads, displacements, and reduced velocities generally increase monotonically with span. Thus, the aeroelastic behavior of the blade is dominated by calculations at 85 and 75 percent span locations. The first harmonic excitation amplitudes calculated by UNSFLO analysis are 37 and 49 percent less for the enlarged rotor-stator spacing compared to the baseline spacing at these two span locations, respectively. The circumferential variation of flow distortion is shown in Figure 27 for the 85 percent span location.

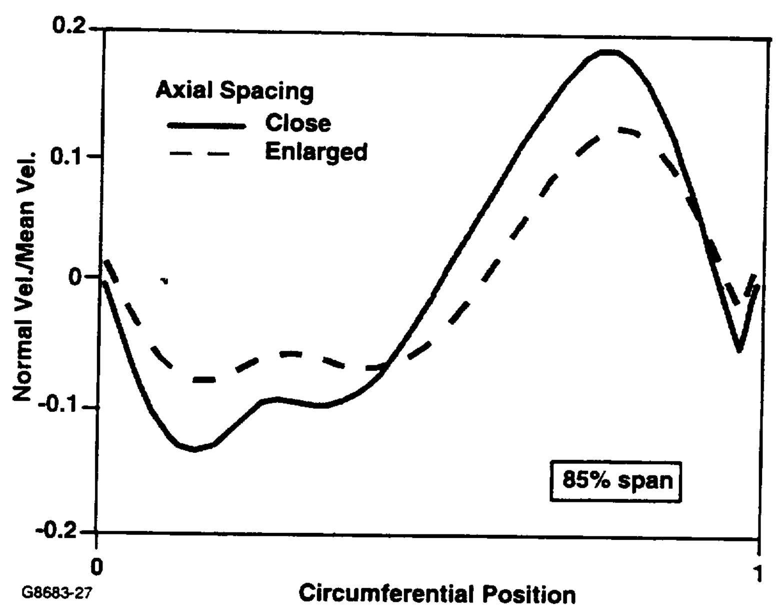

Figure 27. Circumferential Variation Of Flow Distortion.

The modal aeroelastic response of the blade to the excitations in the baseline and the enlarged rotor-stator spacing configurations was calculated as a function of excitation frequency (corresponding to rotor speed). The calculated response reduction due to enlarging the rotor-stator spacing is shown in Figure 28, along with a comparison with test data and UNSFLO calculations. As can clearly be seen, the FREPS predictions are reasonably close to the test data.

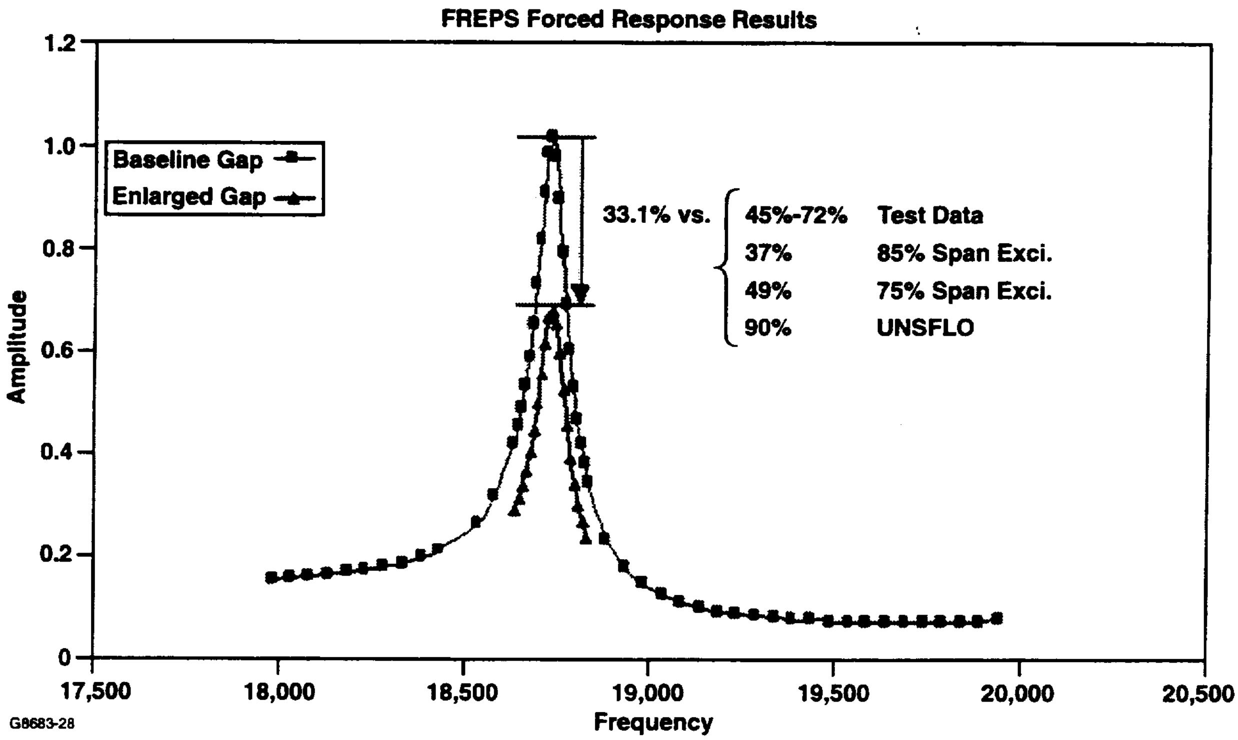

Figure 28. FREPS Response Predictions Compared With Test Data and UNSFLO.

4.3.7 Comments On The FREPS System

The physical modeling in the FREPS system, based on 2-D potential aerodynamics, has been overtaken by more sophisticated models in recent years. However, the greatest strength of the FREPS system is the extremely short computer times required for analysis. Once the input files are generated (including steady flow calculations), aeroelastic analysis with four span locations and one mode at 40 frequencies (as shown for the baseline spacing in Figure 28) can be completed in about 1.5 hours. The response calculation at any given frequency takes about two minutes. However, obtaining convergence for the steady flow calculations is tedious at high speeds and incidence angles, taking away some of the turn-around time advantages. While it is recognized that this is a common problem with two-dimensional aerodynamic codes, AlliedSignal Engines recommends that the steady flow analysis be improved in user friendliness and convergence behavior.

4.4 TURBO-AE Evaluations – HP Turbine Test Case

The TURBO-AE code was evaluated against both an HP turbine test case, for forced response, and a fan blisk test case, for flutter prediction. Both test cases were described previously in section 4.1. The turbine test case simulation is presented in this section, while the fan blisk test case simulation is presented in section 4.5.

4.4.1 General

To evaluate TURBO-AE, AlliedSignal Engines compared experimental observations from a pair of high-pressure (HP) turbine tests with forced response predictions from TURBO-AE and ANSYS®. TURBO-AE was used to characterize the 3-D steady and unsteady flow fields, and ANSYS® was used to predict the turbine blade structural response to this unsteady flow field.

The turbine under investigation, described in section 4.1.1, exhibited significant blade vibratory response due to pressure wakes from upstream stator vanes. Experimental data was collected on two stator-rotor configurations. The first configuration had characteristically close axial spacing and was found to have high vibration levels during testing. The distance separating the trailing and leading edges was approximately 50 percent of the rotor axial tip chord. In the second configuration, vibratory strain levels dropped substantially when the spacing was increased to 70 percent of the rotor axial tip chord.

The two-dimensional UNSFLO and FREPS analyses, presented in sections 4.2 and 4.3 respectively, predicted the right qualitative strain reduction trends, but did not match the strain reductions measured in the testing. Since turbomachinery flows are highly three-dimensional, this investigation used a 3-D, time unsteady, rotor-stator interaction code (TURBO-AE) to investigate the turbine test case. TURBO-AE has better resolution in the spanwise direction than the 2-D analyses. The objective of this analysis is to determine if the TURBO-AE/ANSYS® combination could improve the correlation between experimental observations and analytical predictions.

4.4.2 TURBO-AE Code Description

TURBO-AE was originally developed by Janus, et. al.[10, 11, 12] at Mississippi State University for modeling the flow through multi-stage turbomachinery. It is based on a finite volume scheme. Flux vector splitting is used to evaluate the flux Jacobians on the left-hand side of the governing equations, and Roe's flux difference splitting is used to form a higher-order total variation diminishing (TVD) scheme to evaluate the fluxes on the right-hand side. Newton sub-iterations are used at each time step to maintain accuracy.

Bakhle, et. al.[13, 14] at NASA Lewis Research Center developed routines to interpolate the structural deflections from a finite-element grid to a CFD grid. These routines couple three-dimensional fluid and structural dynamic models to permit flutter analyses. This feature is available for single blade row analyses only. For this reason, blade vibration is not included in the present analyses. The impact of the blade vibration on the unsteady flow solution is not known. Additionally, all analyses presented in this paper are inviscid. Convergence difficulties and excessive computational time precluded viscous analyses. Therefore, TURBO-AE Version 2.0 was used.

4.4.3 Analysis Methodology

TURBO-AE Version 2.0 does not incorporate phase-lag or time-tilt boundary conditions. Such features permit non-integer blade ratios between stator and blade rows. To avoid analyzing the entire rotor, the number of stator vanes was changed from 41 to 39, to obtain a two-to-one ratio between the rotor and stator blades. The computational domain is shown in Figure 29.

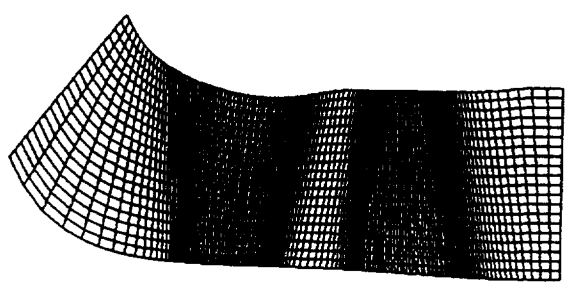

(A) Meridional View.

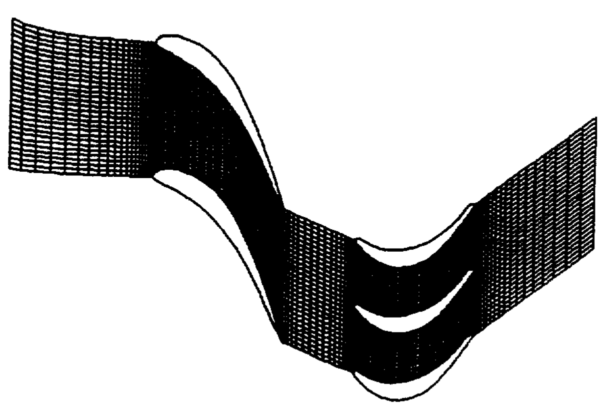

G8683-29 **(B) Blade-To-Blade View.**

Figure 29. Computation Grid For The Flow Field.

The discretization uses single block, sheared H-grids with 81 nodes in the axial direction and 21 nodes in the radial direction. In the circumferential direction, there are 29 nodes for the stator and 15 nodes for the rotor. There are 50 grids from the leading to trailing edges of the turbine blade. A proprietary meshing algorithm was used to create the computational grid. This algorithm uses information about the hub and shroud flow paths, together with sections of the airfoil geometry, to build the computational grid. The airfoil sections can be on the surface of revolution or on a flat surface. The surface of revolution can be a stream line, cylinder, or cone. Computational grids for both the stator and rotor were created separately, and then joined in the tangential direction.

The CFD solution begins with a uniform flow field and a pressure ratio equal to one. Back pressure is gradually decreased to the experimentally measured value. After converging to the correct mass flow rate and pressure ratio, static pressures on the suction and pressure surfaces were written out at fifty equally spaced time intervals in a vane passage period. The unsteady pressures were then mapped onto a finite element model of the blade.

AlliedSignal Engines developed a procedure to map unsteady pressures from a CFD grid to a structural grid and perform a forced-response analysis. In this procedure, unsteady pressures are linearly interpolated between known CFD spans and projected onto the structural grid at equally-spaced time intervals in a single vane passage period.

In the HP turbine test case, the vane passage period was broken into fifty equally-spaced time steps. For each time step, pressures on the pressure and suction surfaces of the blade were imported into the structural model and projected onto a truncated number of structural finite element modes. A transient, forced-response analysis was conducted by repeatedly feeding the excitation from the vane passage period to the finite element model until the transient response diminished. The resulting steady-state solution yielded the maximum vibratory strain experienced by the blade. The forced response analysis could also have been done as a modal system.

4.4.4 TURBO-AE HP Turbine Test Case Results

Unsteady flow solutions were obtained for three different stator-rotor configurations. Two of the stator-rotor configurations correspond to the experimental investigation, with 50 and 70 percent chord spacing, respectively. The third configuration corresponds to 25 percent chord spacing. The static pressure envelope at mid-span for each of the spacing configurations is shown in Figure 30.

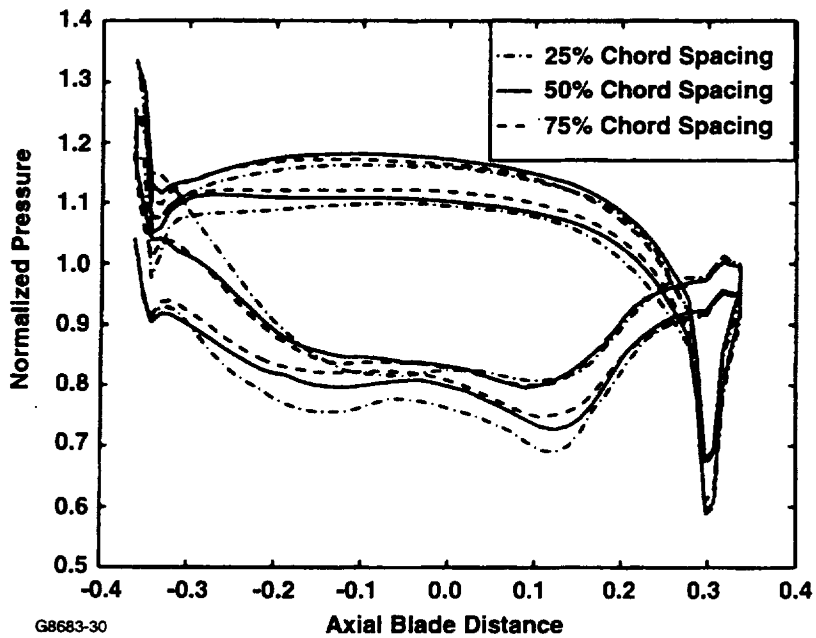

Figure 30. Static Pressure Envelope At 50 Percent Span.

The envelope conveys the maximum and minimum static pressure variation on the rotor airfoil as the blades pass through one pitch of the upstream stator. The pressure fluctuation is highest in the leading edge area, but is present throughout by the airfoil surface. On the suction surface, there is an adverse pressure gradient near the leading edge region. The gradient is due to the negative incidence of the flow. The fluctuation is greatest for the close spacing configuration. Figure 31 shows the unsteady pressure fluctuation contours at four intermediate times for the 50 percent chord spacing case. The contours consist of the unsteady pressure minus the steady-state pressure. Pressure waves created by the upstream stator are clearly seen in Figure 31.

As stated earlier, the forced response analyses consisted of importing unsteady pressures from TURBO-AE for a single vane passage period and repeatedly feeding the pressure description to a structural finite element model until the transient response diminishes. The vibratory response and spectra of the 50 and 70 percent chord spacing solutions are shown in Figures 32 and 33, respectively. The magnitude of the strains do not differ significantly. The inviscid based analyses capture potential effects which are significant when the stator and rotor blades are in close proximity to each other, not when the blades are well separated. Figure 34 illustrates a spacing configuration in which the distance separating trailing and leading edges is 25 percent of the rotor tip chord. Strain levels increased 54 percent over the 50 percent chord solution. A critical damping ratio of 2.0 percent was used in all the analyses.

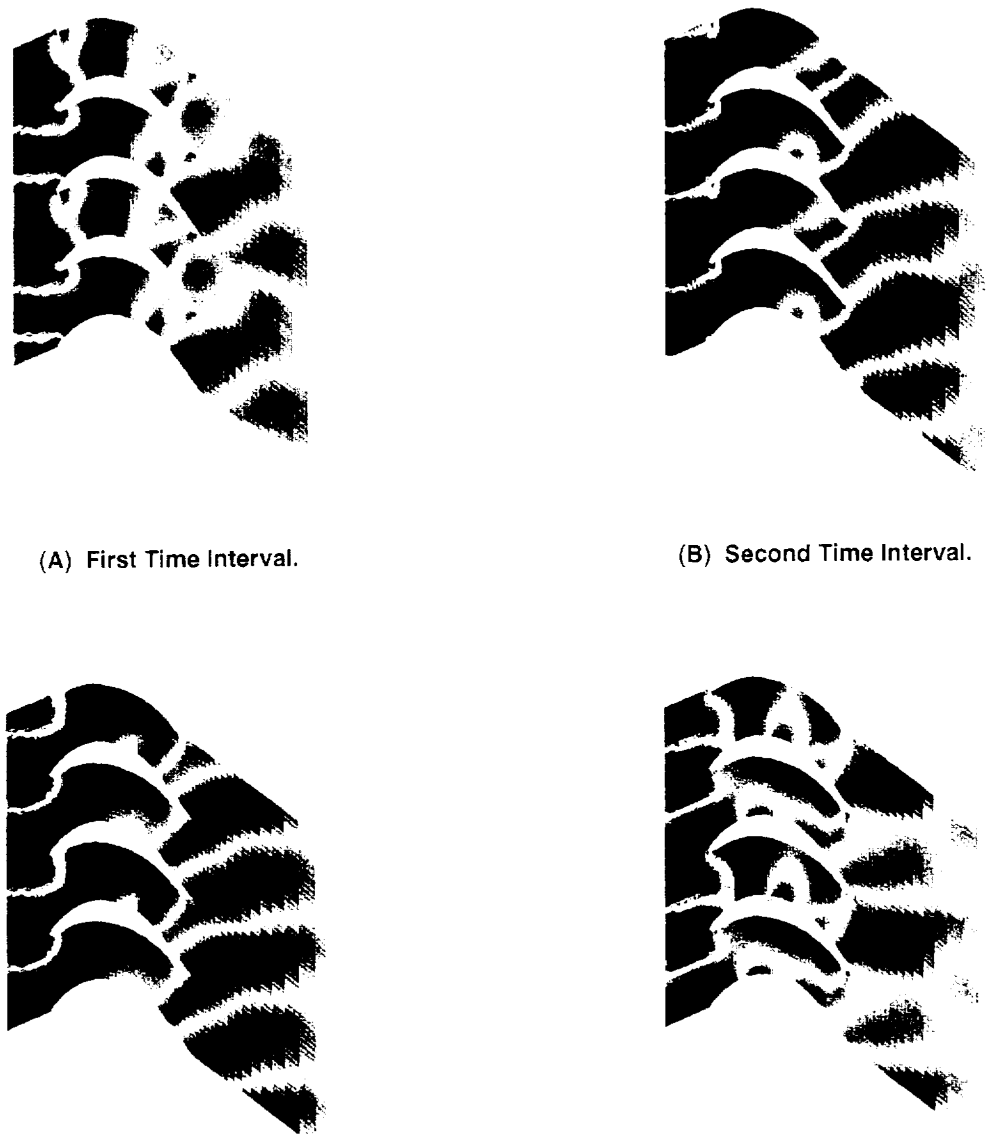

(A) First Time Interval.

(B) Second Time Interval.

(C) Third Time Interval.

(D) Fourth Time Interval

G8683-31

Figure 31. Unsteady Pressure Contours At Four Equally-Spaced Time Intervals In A Vane Passage Period.

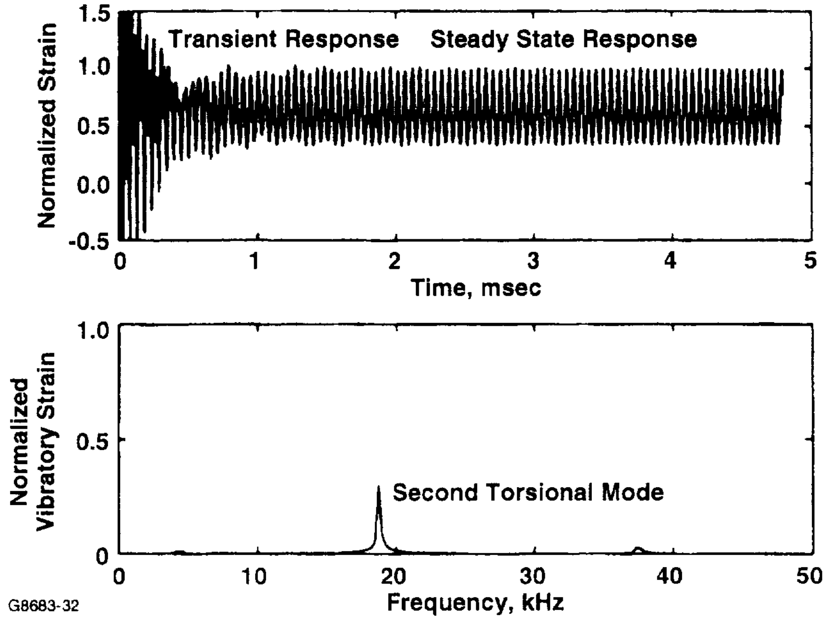

Figure 32. Vibratory Response And Spectrum For 50 Percent Chord Spacing.

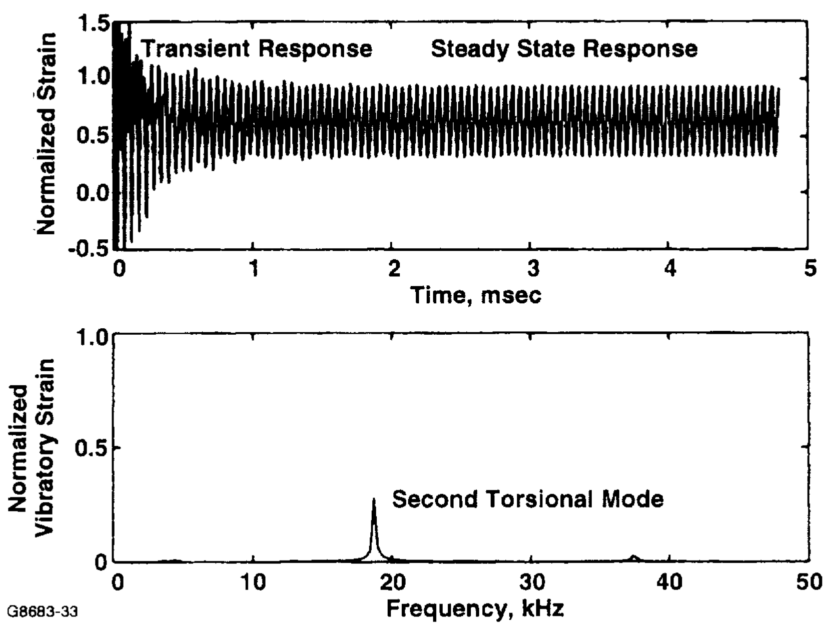

Figure 33. Vibratory Response And Spectrum For 70 Percent Chord Spacing.

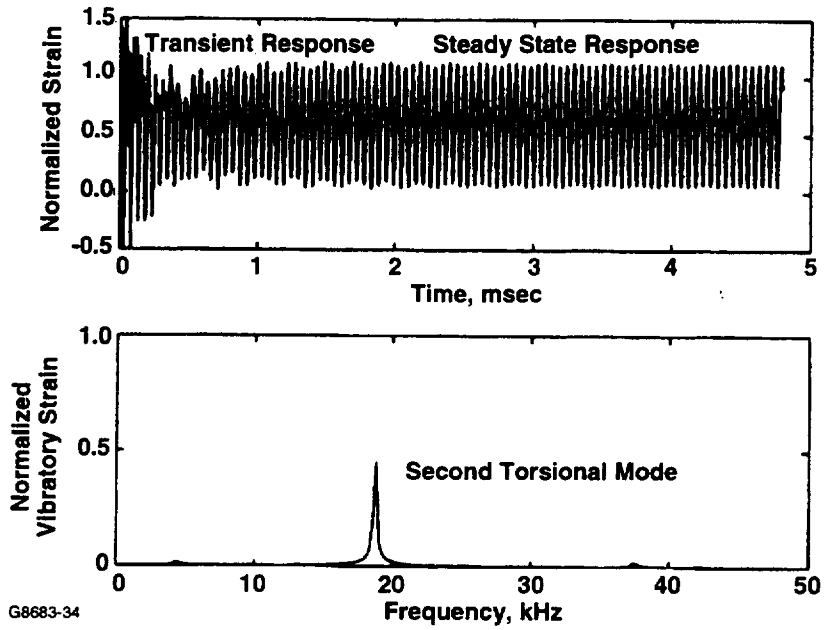

Figure 34. Vibratory Response And Spectrum For 25 Percent Chord Spacing.

4.4.5 Conclusions – TURBO-AE HP Turbine Test Case

For the high-pressure (HP) turbine test case, strain reductions from 45 to 72 percent were measured when the axial space between stator and rotor blades was increased from 50 to 70 percent of the rotor axial tip chord. Three inviscid TURBO-AE analyses were performed with spacings of 25, 50, and 70 percent chord. Appreciable strain level differences did not occur until the spacing distance was reduced to 25 percent of the rotor chord. Potential effects captured by the inviscid analyses are pronounced when the rotor and stator blades are in close proximity to each other, not when they are well separated. Viscous effects dominate the 50 and 70 percent chord spacings and three dimensional viscous analyses are needed.

4.5 TURBO-AE Evaluation -- Fan Blisk Test Case

The TURBO-AE code was evaluated against both the HP turbine test case, for forced response, and the fan blisk test case, for flutter prediction. Both test cases are described in section 4.1. The fan test case simulation is presented in this section, while the HP turbine test case simulation is presented in section 4.4.

4.5.1 General

The goal for the fan blisk test case was the evaluation of the currently available version of the TURBO-AE code. We planned to evaluate a number of flutter and non-flutter test cases with the TURBO-AE code. These flutter (F1 through F6) and non-flutter (NF1 and NF2) test conditions for which test data was available are shown in the fan performance map of Figure 35. The F2 test case was chosen as the initial case, to capitalize on work performed previously by AlliedSignal Engines under the NASA-sponsored Small Engine Technology (SET) Task 8 program.

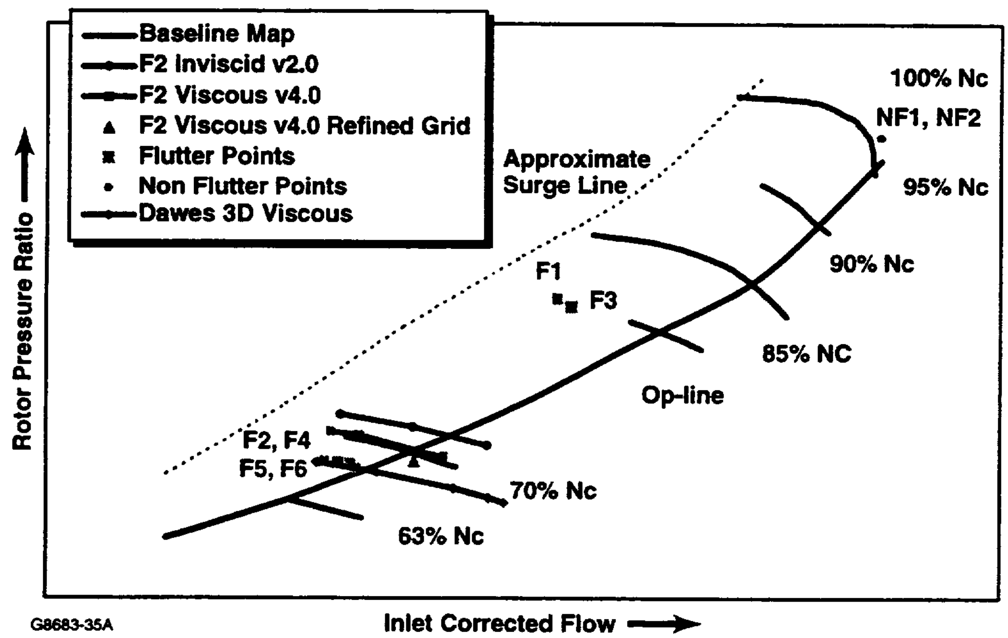

Figure 35. AE Fan Blisk Rotor Test And Computational Results.

A copy of the Preliminary Version 4.0 TURBO-AE code was made available to AlliedSignal Engines in the third quarter of 1997. Subsequently, the Final Version 4.0 TURBO-AE code was made available in the first quarter of 1998. The Preliminary Version 4.0 TURBO-AE code provided us with viscous analysis capability and incorporated the use of time- (or phase-) shifted boundary conditions – an option that was not functional in the Version 2.0 code supplied to AE during the NASA SET Task 8 program. Additionally, the Final Version 4.0 TURBO-AE program incorporated the use of the non-reflecting inlet and exit boundary conditions. NASA also supplied computer time on their CRAY C90 machine to run the test cases for the fan blisk test case.

4.5.2 TURBO-AE Code Description

The aeroelastic analysis code TURBO-AE is under development at NASA Lewis Research Center.[13] The starting point for the development was an Euler/Navier-Stokes unsteady aerodynamic code named TURBO which was generated at Mississippi State University.[10, 15] Routines have been developed to interpolate the structural deflections from the finite-element grid to the CFD grid to capture the blade motion in the analysis. Grid deformation routines have been developed to calculate a new grid for the deformed blade at each time step. Routines have been developed for the calculation of work and generalized forces. These routines have been verified by running the code for a standard configuration.

The TURBO code was originally developed as an inviscid flow solver for modeling the flow through multistage turbomachinery. It has the capability to handle multiple blade rows with even or uneven blade count and stationary or rotating blade rows. Additional developments were made to incorporate viscous terms into the model. The code can now be applied to model realistic turbomachinery configurations with flow phenomena such as shocks, vortices, separated flow, secondary flows, and shock and boundary layer interactions.

TURBO is based on a finite volume scheme. Flux vector splitting is used to evaluate the flux Jacobians on the left hand side of the governing equations and Roe's flux difference splitting is used to form a higher-order TVD (Total Variation Diminishing) scheme to evaluate the fluxes on the right hand side. Newton sub-iterations are used at each time step to maintain higher accuracy. A Baldwin-Lomax algebraic turbulence model is used in the code.

The TURBO-AE code assumes a normal mode representation of the structural dynamics of the blade. Thus, the dynamic characteristics of each blade are assumed to be represented in terms of structural modes, with the associated natural frequency and generalized mass for each mode. Typically, a finite-element analysis code such as ANSYS is used to calculate the modal behavior mentioned.

A work-per-cycle approach is used to determine aeroelastic (flutter) stability. Using this approach, the motion of the blade is prescribed to be a harmonic vibration in a specified normal mode with a specified frequency. The vibration frequency is typically the natural frequency for the mode of interest, but some other frequency can also be used. The aerodynamic forces acting on the vibrating blade and the work done by these forces on the vibrating blade during a cycle of vibration are calculated. If work is being done on the blade by the aerodynamic forces, the blade is dynamically unstable, since it will result in extraction of energy from the flow, leading to an increase in amplitude of oscillation of the blade. Note that coupled mode flutter cannot be modeled with this approach.

The current release of the TURBO-AE code is capable of evaluating arbitrary inter-blade phase angles using a single blade passage. This is accomplished by using a single blade passage with time (or phase) shifted boundary conditions.

4.5.3 Flutter Vibrations on F2 Test Case

The F2 test case was selected as the starting point for evaluating the 4.0 version of the TURBO-AE code. The F2 test case was the initial case evaluated during the NASA SET Task 8 program and computational results were readily available. The computational grids used during the analyses are shown in Figures 36 and 37. The first grid is the same grid used during the SET Task 8 program. This coarse grid (90 x 35 x 25) is coarser than grids typically used for viscous analyses. The second, more refined grid is reflective of a viscous computational grid (120 x 67 x 33). Unlike the first grid, the second grid also has incorporated into the geometric definition a shroud clearance gap of 0.19 percent gap-to-blade height. The clearance gap was constructed using four volume cells.

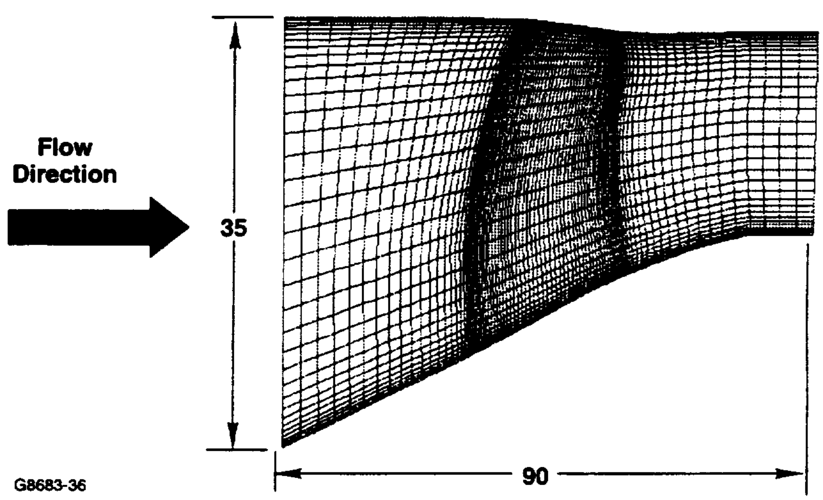

Figure 36. Coarsė Computational Grid For TURBO-AE Analyses.

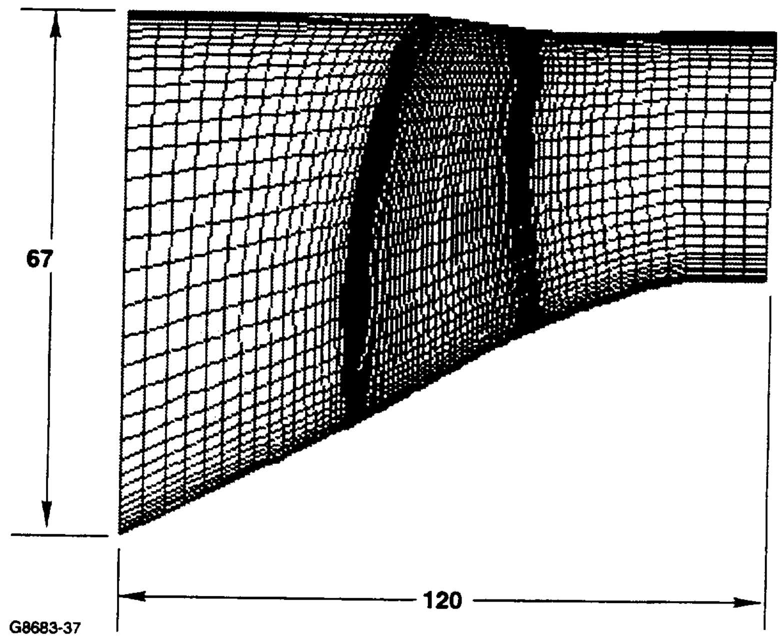

Figure 37. Refined Computational Grid For TURBO-AE Analyses.

4.5.4 Analysis Results

Upon receipt of the preliminary version of the TURBO-AE code, a baseline check of the code was made by re-running one of the F2 inviscid runs performed during the NASA SET Task 8 program. The results compared favorably. The next step in the evaluation process was to generate a viscous solution representative of the steady-state F2 data for the fan blisk test case. This step was performed utilizing two viscous configurations. The first configuration was a rerun of the F2 cases evaluated during the NASA SET Task 8 program, utilizing the viscous capabilities of the 4.0 version of the TURBO-AE code. The computational grid used for the first configuration is shown in Figure 36. The grid size (90 x 35 x 25) is generally considered to be a coarse grid, not normally used for viscous analysis. The impact of the viscous effects on the fan blisk pressure ratio versus flow characteristic is clearly obvious in Figure 35. The constant corrected speed characteristic shifted towards lower pressure ratio and flow, a trend typically seen between a viscous and inviscid comparison.

A more detailed look at the blade static pressure rise loading for 30 and 90 percent spans, Figures 38 and 39, respectively, also indicates the benefit of the viscous terms in the analysis. The shock wave location and strength is altered between the viscous and inviscid solutions. The shock wave strength is diminished and moved toward the leading edge of the blade. If the flutter characteristics of the fan blisk are related to the starting and unstarting of the compressor blade row, then proper modeling of the location and strength of the imbedded shock wave will be important to the unsteady solution.

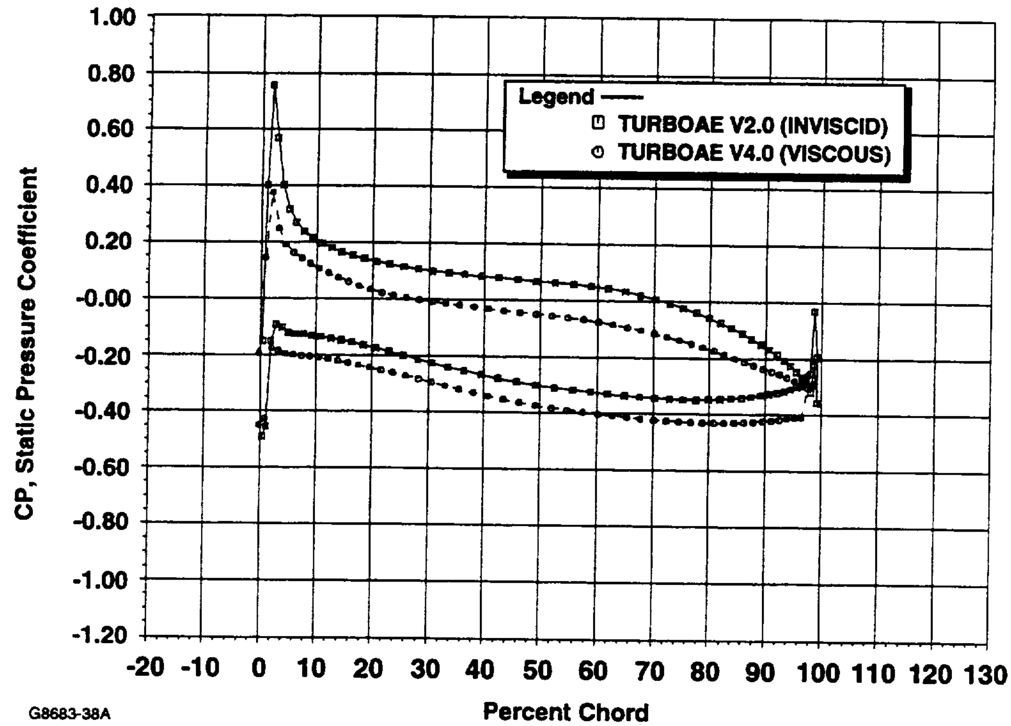

Figure 38. Steady Flow TURBO-AE Viscous/Inviscid Comparison for Case F2 at 30 Percent Span.

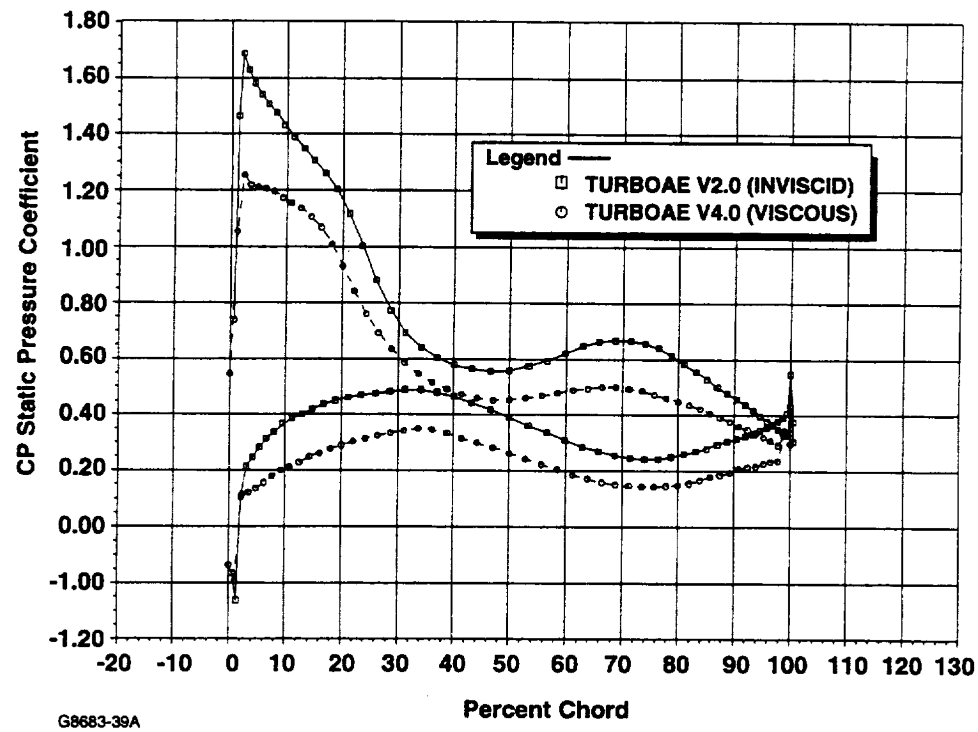

Figure 39. Steady Flow TURBO-AE Viscous/Inviscid Comparison for Case F2 at 90 Percent Span.

The second configuration involved a viscous analysis with a more refined computational grid. The computational grid size was increased to be more representative of a viscous type grid. The overall grid size was increased from 78,750 grid nodes to 265,320 nodes. The refined grid is shown in Figure 37. The grid clustering was increased in the leading and trailing edge regions to provide better blade definition in the high-curvature regions. The refined grid also incorporated a clearance gap model. It was felt that the clearance gap would be important to the unsteady analysis, since it impacts the blade tip flow structure. The clearance gap also eliminates the unsteady work that would be attributed to the blade if it were modeled without a clearance gap. During the unsteady analysis, the highest deflections for this geometry occurs at the blade tip; thus, any type of blade loading would be generating unsteady work that realistically is not present, due to the clearance gap.

During the course of evaluating the refined grid configuration, a number of difficulties were encountered. An attempt to use the multi-block gridding capability of TURBO-AE met with little success. Thus, the size of the grid as a single block limited access to the CRAY machines. It was eventually determined that the input parameters for the multi-block gridding were being specified incorrectly. It was also necessary to experiment with some of the CFD input parameters in order to achieve successful execution of TURBO-AE.

The parameters investigated were ITEND (number of refinement iterations, default = 3) and NBC_MODES (number of circumferential Fourier modes, default = 2). Various combinations of ITEND and NBC_MODES were tested, and the only combination found to work was ITEND = 1 and NBC_MODES = 0. It is not clear to AlliedSignal what impact these parameters may have on the steady or unsteady solutions. Convergence problems were also encountered, as a result of how the blade row back pressure is specified. After some investigation, it was determined that the interpretation of how NBPD (number of time steps for which gradual back pressure increase is used) and PRAT (pressure ratio, exit to inlet) are used differs, based on the IOBC_OPT (inlet/exit boundary condition flag). After resolving these issues, a converged data point was achieved for the refined grid.

The refined grid required 8,000 iterations for convergence at approximately 1,000 iterations per 8 hours of execution time. This was an increase in execution time of approximately 300 percent beyond that required for the coarse viscous grid. The impact of the refined grid on the fan map characteristic can be seen in Figure 35. Increasing the grid density and including a clearance gap also reduces the pressure ratio and inlet corrected flow for the fan rotor. This new grid configuration compares more favorably to the tested results than did the previous inviscid configuration evaluated with TURBO-AE during the NASA SET Task 8 effort at AlliedSignal Engines. Also included in Figure 35 are the DAWES viscous cases, using the same refined viscous grid with the clearance gap. The agreement between the tested results and the DAWES data is excellent.

Comparison of the coarse grid viscous results with the refined grid reveals some of the benefits of using a finer grid. At 30 percent span, the agreement between the coarse and refined grids is remarkably similar (Figure 40). The refined grid indicates a lower loading level at this span section, and a higher peak velocity on the suction surface. At 90 percent span, the refined grid has a much higher peak velocity on the suction surface and better definition (Figure 41). The higher peak velocity on the suction surface is attributed to the increased grid resolution in the leading edge region. The overall strength and sharpness of the shock wave was increased for the refined grid.

The changes made to the computational grid and the inclusion of viscous effects have been demonstrated to have a substantial impact on the resulting steady-state solution. Such influences can have significant impact on the TURBO-AE unsteady execution, inasmuch as the steady-state solution is the initial condition for the unsteady analysis.

As described in section 4.5.5 above, significant effort was expended by AlliedSignal Engines in getting the viscous version of the TURBO-AE code to give converged, steady flow solutions for the transonic flow conditions in the fan blisk. Once converged, steady solutions provided an improved match with test data. Due to the effort required to understand and resolve the difficulties encountered with the steady-state solutions, no unsteady runs of the TURBO-AE code were completed.

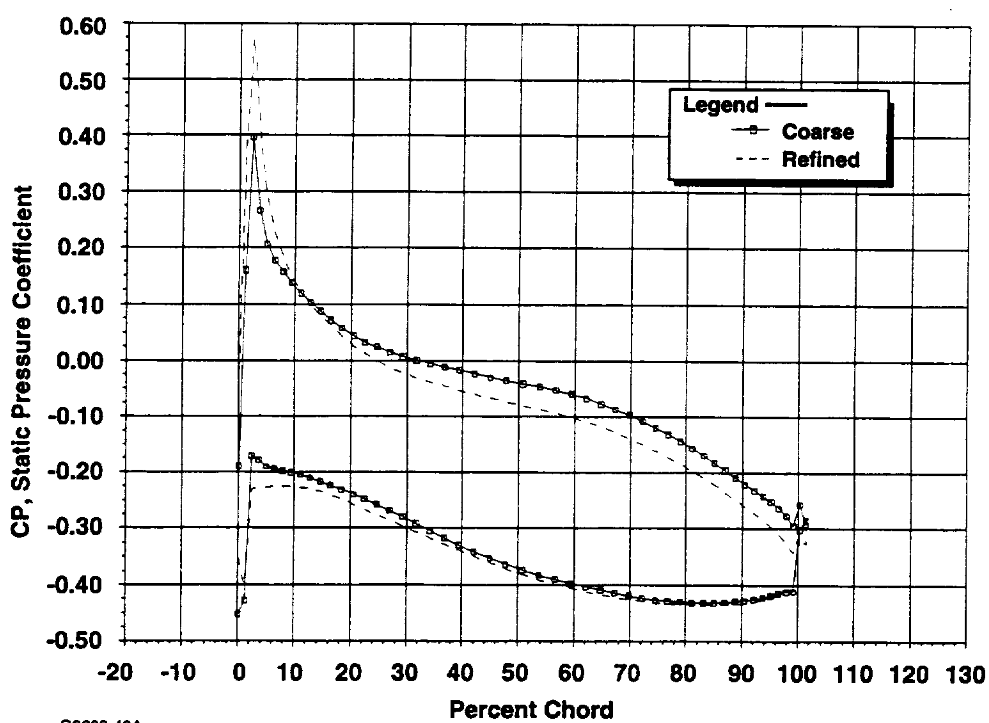

Figure 40. Steady Flow TURBO-AE Coarse/Refined Grid Comparison for Case F2 at 30 Percent Span.

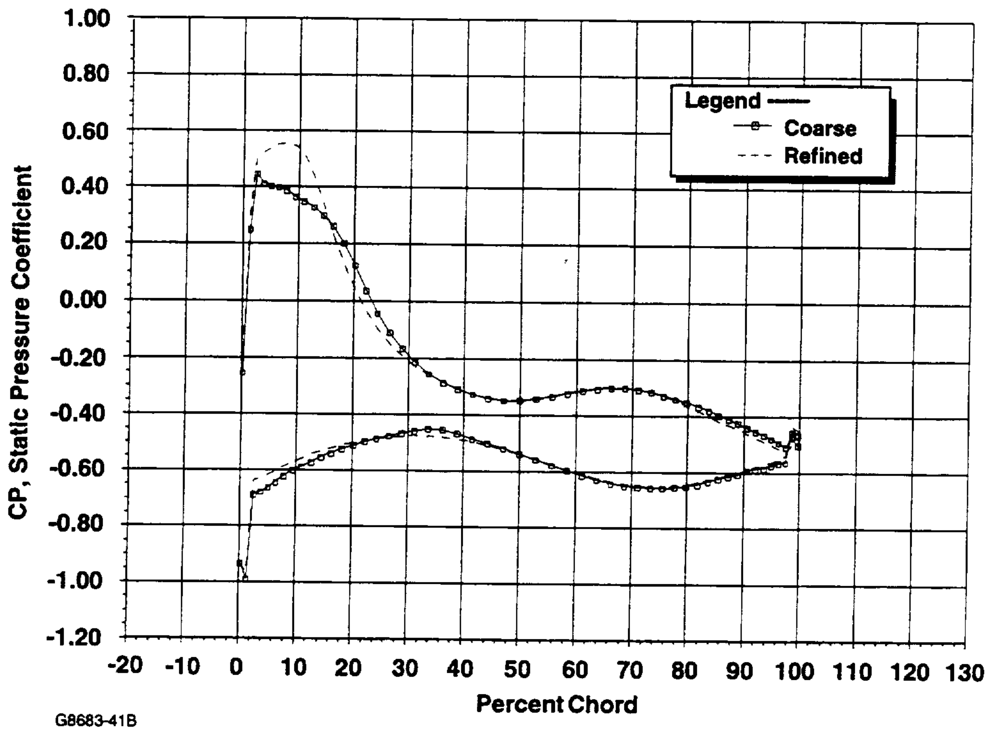

Figure 41. Steady Flow TURBO-AE Coarse/Refined Grid Comparison for Case F2 at 90 Percent Span.

4.5.5 Recommendations for Further Development of the TURBO-AE Code

During the course of applying TURBO-AE on the HP turbine and fan blisk test cases, AlliedSignal Engines obtained substantial experience operating the TURBO-AE code. Several areas for improvement and further study have been suggested and are summarized as follows:

- Improvements are needed in initializing the unsteady solution. A capability to start from an APNASA steady solution would be ideal.
- The specification of inlet boundary conditions in terms of Mach number and pressure ratio is not appropriate for turbomachinery applications. Specification of inlet total temperature and total pressure is more appropriate.
- The specification of overall pressure ratio should be more robust so less manual intervention is required to maintain numerical stability.
- Improvements are needed in the convergence monitoring capability. Provide the capability to monitor program convergence during execution.
- A parallel processing capability with a generalized multi-block grid (radial and tangential) would speed solution times.

- During the on-going consolidation of the various versions of TURBO and TURBO-AE, the aeroelastic features currently in TURBO-AE should be tightly coupled with the TURBO code to minimize solution times.
- A capability to model purge flow source terms is needed.

TURBO-AE is an important component of the AlliedSignal technology and tool development plan, expecting it to play a key role in the development of new turbomachinery. AlliedSignal Engines is grateful to NASA-Lewis for the leadership shown in the development of the TURBO/TURBO-AE codes and we are hopeful it will continue a sustained focus for further code consolidation and development.

5. SUMMARY

During the course of the NASA Advanced Subsonic Technology (AST) program Area of Interest (AOI) 6 (from November, 1996 through September, 1998) AlliedSignal Engines made significant progress toward the goals of validating CFD-based aeroelastic analysis tools and upgrading our design tools to include these analyses. Prior to 1995, all aeroelastic analyses at AE had been completed using only empirical correlations; while we now have the capability to complete substantially more detailed analyses.

This work demonstrated the successful integration of the UNSFLO, FREPS, and TURBO-AE codes with the structural dynamics code ANSYS®. It is recognized that there are limitations on the level of physics modeling that is included with each of these CFD codes. However, it is still felt that comparing predictions from these codes with actual test data is beneficial. Such an evaluation requires the development of all associated methodology, and a key development of this program is an integrated aeroelastic prediction system. The evaluation also quantifies the contributions to the blade response of the physical flow phenomena that are captured. As advancements are made in the sophistication of the modeling of the unsteady aerodynamics, these improved tools can be incorporated into the aeroelastic design system.

Analyses were conducted for each of the three CFD codes for the case of vane passing for a high-pressure turbine test case. UNSFLO simulations of two axial stator-rotor spacing configurations, at 50 and 70 percent of the turbine rotor axial tip chord, indicate a 90 percent reduction in vibratory strain. The software predictions agree favorably with experimental observations, which showed a 45 to 72 percent reduction in vibratory strain. UNSFLO is establishing itself as a useful design tool for investigating rotor-stator interaction effects.

FREPS simulations of the two turbine stator-rotor spacing configurations indicate a 33 percent reduction in vibratory strain, and a 37 and 49 percent reduction in the first harmonic excitation amplitudes at the 85 and 75 percent span locations, respectively. The code predictions agree favorably with experimental observations showing a 45 to 72 percent reduction in vibratory strain. Although physical modeling in the FREPS system, based on two-dimensional (2-D) potential aerodynamics, has been overtaken by more sophisticated models in recent years, the greatest strength of FREPS is the extremely short computer times required for analysis. However, obtaining convergence for the steady flow calculations is tedious at high speeds and incidence angles, taking away some of the turn-around time advantages.

Three inviscid TURBO-AE analyses were performed on the HP turbine test case, with spacings of 25, 50, and 70 percent chord, respectively. Appreciable strain level differences did not occur until the spacing distance was reduced to 25 percent of the rotor chord. Potential effects captured by the inviscid analyses are pronounced when the rotor and stator blades are in close proximity to each other, but not when they are well separated. Viscous effects dominate the 50 and 70 percent chord spacings, and three-dimensional (3-D) viscous analyses are needed.

For the fan blisk test case, a considerable number of difficulties were encountered while trying to establish a more realistic steady-state simulation with the Final Version 4.0 TURBO-AE code. These difficulties were overcome, and the impact of modeling viscous effects, grid generation, and clearance effects were made clear. Unfortunately, the efforts performed by AE in establishing a representative steady-state solution prevented our exercising the unsteady flutter portion of the TURBO-AE code.

The work performed by AlliedSignal Engines under this program has demonstrated that current computational fluid dynamics (CFD) codes can predict the aeroelastic implications of various design changes; and that integration of two previously autonomous fields, computational fluid dynamics and structural dynamics, will aid future turbomachinery designs.

6. REFERENCES

(1) Eick, C. D., and Liu, J-S, NASA Small Engine Technology (SET) Task 8: Aeroelastic Prediction Methods Final Report (Contract No. NAS3-27483), NASA Report No. CR-202328, AlliedSignal Engines Report No. 21-9527; Prepared for NASA Lewis Research Center, Cleveland, OH; AlliedSignal Engines, Phoenix, AZ, December, 1996.

(2) Richardson, S. M., and Griffin, J. H., "The GUIde Consortium: Government, Universities, and Industry Working Together to Develop New Technologies," ASME Paper 95-GT-278, Proceedings of the 1995 ASME International Gas Turbine and Aeroengine Congress and Exposition, Houston, TX. American Society of Mechanical Engineers, 1995.

(3) (Anonymous), ANSYS Users Manual, Volume IV, "Theory", 1st Revision, September 30, 1994, ANSYS, Inc., Canonsburg, PA; refer to the ANSYS website on the World Wide Web at the URL: **http://www.ansys.com/**

(4) Giles, M. B., "UNSFLO: A Numerical Method for the Calculation of Unsteady Flow in Turbomachinery," MIT Gas Turbine Laboratory Report, 1991, Massachusetts Institute of Technology, Cambridge, MA 02139.

(5) Giles, M. B. and Haimes, R. "Validation of a Numerical Method for Unsteady Flow Calculations," ASME Journal of Turbomachinery, Vol. 115, pp. 110-117, 1993, American Society of Mechanical Engineers.

(6) Abhari, R. S., Guenette, G. R., Epstein, A. H., and Giles, M. B., "Comparison of Time-Resolved Turbine Rotor Blade Heat Transfer Measurements and Numerical Calculations," ASME Paper 91-GT-268; Transactions of the ASME, Vol. 114, p. 818, October, 1992. American Society of Mechanical Engineers.

(7) Morel, M. R., and Murthy, D. V., Turbomachinery Forced Response Prediction System; (FREPS) Users Manual, NASA CR-194465, March, 1994, NASA Lewis Research Center, Cleveland, OH.

(8) Murthy, D. V., Stefko, G. L., and More, M. R., "Forced Response Prediction System (FREPS) for Turbomachinery," presented at the 1994 Conference on Advanced Earth-to-Orbit Propulsion Technology and Exhibit, NASA Marshall Spaceflight Center, Huntsville, AL, May, 1994.

(9) McCormick, C. W., ed.; MSC/NASTRAN Users Manual, Vol. I and II, MacNeal-Schwendler, Los Angeles, CA 1983.

(10) Janus, J. M., "Advanced 3-D CFD Algorithm for Turbomachinery, " Ph.D. Dissertation, 1989, Mississippi State University, Mississippi State, MS 39762.

(11) Janus, J. M., and Whitfield, D. L., "A Simple Time-Accurate Turbomachinery Algorithm with Numerical Solutions of an Uneven Blade Count Configuration," AIAA Paper 89-0206, January, 1989, American Institute of Aeronautics and Astronautics.

(12) Chen, J. P., and Whitfield, D. L., "Navier-Stokes Calculations for the Unsteady Flowfield of Turbomachinery," AIAA Paper 93-0676, January, 1993, American Institute of Aeronautics and Astronautics.

(13) Bakhle, M. A., et. al., "Development of an Aeroelastic Code Based on an Euler/Navier-Stokes Aerodynamic Solver, " ASME Paper 96-GT-311, 1996, American Society of Mechanical Engineers.

(14) Bakhle, M. A., et. al., "A 3D Euler/Navier-Stokes Aeroelastic Code for Propulsion Applications," AIAA Paper 97-2749, July, 1997, American Institute of Aeronautics and Astronautics.

(15) Chen, J. P., "Unsteady Three-Dimensional Thin-Layer Navier-Stokes Solutions for Turbomachinery in Transonic Flow," Ph.D. Dissertation, 1991, Mississippi State University, Mississippi State, MS 39762.

REPORT DOCUMENTATION PAGE

Form Approved
OMB No. 0704-0188

1. AGENCY USE ONLY (*Leave blank*)	2. REPORT DATE	3. REPORT TYPE AND DATES COVERED
	September 1999	Final Contractor Report

4. TITLE AND SUBTITLE

Advanced Subsonic Technology (AST) Area of Interest (AOI) 6: Develop and Validate Aeroleastic Codes for Turbomachinery

5. FUNDING NUMBERS

WU-538-12-10-00
NAS3-27752

6. AUTHOR(S)

Kevin D. Gardner, Jong-Shang Liu, Durbha V. Murthy, Marlin J. Kruse, and Darrell James

7. PERFORMING ORGANIZATION NAME(S) AND ADDRESS(ES)

AlliedSignal Engines
111 S. 34th Street
P.O. Box 85072-2180
Phoenix, Arizona 85072-2180

8. PERFORMING ORGANIZATION REPORT NUMBER

E-11933

9. SPONSORING/MONITORING AGENCY NAME(S) AND ADDRESS(ES)

National Aeronautics and Space Administration
John H. Glenn Research Center at Lewis Field
Cleveland, Ohio 44135-3191

10. SPONSORING/MONITORING AGENCY REPORT NUMBER

NASA CR—1999-209406
ASE 21-10345

11. SUPPLEMENTARY NOTES

Project Manager, David Janetzke, Structures and Acoustics Division, NASA Glenn Research Center, organization code 5930, (216) 433-6041.

12a. DISTRIBUTION/AVAILABILITY STATEMENT

Unclassified - Unlimited
Subject Category: 07 Distribution: Nonstandard

This publication is available from the NASA Center for AeroSpace Information, (301) 621-0390.

12b. DISTRIBUTION CODE

13. ABSTRACT *(Maximum 200 words)*

AlliedSignal Engines, in cooperation with NASA GRC, completed an evaluation of recently-developed aeroelastic computer codes using test cases from the AlliedSignal Engines fan blisk and turbine databases. Test data included strain gage, performance, and steady-state pressure information obtained for conditions where synchronous or flutter vibratory conditions were found to occur. Aeroelastic codes evaluated included quasi 3-D UNSFLO, 2-D FREPS, and 3-D TURBO-AE. Unsteady pressure predictions for the turbine test case were used to evaluate the forced response prediction capabilities of each of the three aeroelastic codes. Additionally, one of the fan flutter cases was evaluated using TURBO-AE. The UNSFLO and FREPS evaluation predictions showed good agreement with the experimental test data trends, but quantitative improvements are needed. UNSFLO over-predicted turbine blade response reductions, while FREPS under-predicted them. The inviscid TURBO-AE turbine analysis predicted no discernible blade response reduction, indicating the necessity of including viscous effects for this test case. For the TURBO-AE fan blisk test case, significant effort was expended getting the viscous version of the code to give converged steady flow solutions for the transonic flow conditions. Once converged, the steady solutions provided an excellent match with test data and the calibrated DAWES 3-D viscous solver. However, efforts expended establishing quality steady-state solutions prevented exercising the unsteady portion of the TURBO-AE code during the present program. AlliedSignal recommends that unsteady pressure measurement data be obtained for both test cases examined for use in aeroelastic code validation.

14. SUBJECT TERMS

Aeroelasticity; Fan blisk; CFD

15. NUMBER OF PAGES

60

16. PRICE CODE

A04

17. SECURITY CLASSIFICATION OF REPORT	18. SECURITY CLASSIFICATION OF THIS PAGE	19. SECURITY CLASSIFICATION OF ABSTRACT	20. LIMITATION OF ABSTRACT
Unclassified	Unclassified	Unclassified	

NSN 7540-01-280-5500

Standard Form 298 (Rev. 2-89)
Prescribed by ANSI Std. Z39-18
298-102